https://doi.org/10.5194/cp-2021-106
Preprint. Discussion started: 10 September 2021
© Author(s) 2021. CC BY 4.0 License.

Climate of the Past Discussions

Late Pleistocene glacial chronologies and paleoclimate in the northern Rocky Mountains

Brendon J. Quirk[1*], Elizabeth Huss[2], Benjamin J.C. Laabs[3], Eric Leonard[4], Joseph Licciardi[5], Mitchell A. Plummer[6], Marc W. Caffee[7]

[1] Department of Geology and Geophysics, University of Utah, Salt Lake City, Utah 84112, USA

[2]Department of Geosciences, State University of New York at Geneseo, Geneseo, NY 14454, USA

[3]Department of Geosciences, North Dakota State University, Fargo, North Dakota 68102, USA

[4]Department of Geology, Colorado College, Colorado Springs, Colorado 80903, USA

[5]Department of Earth Sciences, University of New Hampshire, Durham, New Hampshire 03824, USA

[6]Idaho National Engineering and Environmental Laboratory, Idaho Falls, Idaho 83415, USA

[7]Department of Physics, PRIME Lab, Purdue University, West Lafayette, Indiana 47905, USA

[*]Corresponding author email address: bjquirk@purdue.edu

ABSTRACT

The geologic record of mountain glaciations is a robust indicator of terrestrial paleoclimate change. During the last glaciation, mountain ranges across the western U.S. hosted glaciers while the Cordilleran and Laurentide ice sheets flowed to the west and east of the continental divide, respectively. Records detailing the chronologies and paleoclimate significance of these ice advances have been developed for many sites across North America. However, relatively few glacial records have been developed for mountain glaciers in the northern Rocky Mountains near ice sheet margins. Here, we report cosmogenic beryllium-10 surface exposure ages and numerical glacier modeling results showing that mountain glaciers in the northern Rockies

https://doi.org/10.5194/cp-2021-106
Preprint. Discussion started: 10 September 2021
© Author(s) 2021. CC BY 4.0 License.

Climate of the Past Discussions

abandoned terminal moraines after the end of the Last Glacial Maximum around 17-18 ka and could have been sustained by -10 to -8.5°C temperature depressions relative to modern assuming similar or drier than modern precipitation. Additionally, we present a deglacial chronology from the northern Rocky Mountains that indicates while there is considerable variability in initial moraine abandonment ages across the Rocky Mountains, the pace of subsequent ice retreat through the Lateglacial exhibits some regional coherence. Our results provide insight on potential regional mechanisms driving the initiation of and sustained deglaciation in the western U.S. including rising atmospheric CO_2 and ice sheet collapse.

INTRODUCTION

Mountain glaciers are widely recognized as robust indicators of modern climate change (Oerlemans, 2005; Vaughan et al., 2013; Mark and Fernández, 2017). Investigations of past glacier fluctuations preserved in the geologic record can therefore reveal valuable information regarding past climate oscillations and variability (e.g. Gilbert, 1890; Blackwelder, 1931; McCoy et al., 1985; Marcott et al., 2019). In the Rocky Mountain region of the western U.S. records of mountain glaciation have been used extensively to reconstruct the regional pattern of Pleistocene glaciation in space and time (e.g., Porter et al., 1983; Leonard, 1989; Licciardi et al., 2004; Laabs et al., 2009; Quirk et al., 2020), but few studies have focused on northern ranges along the former southern margins of the Laurentide and Cordilleran ice sheets. While surficial geologic records of Pleistocene mountain glaciation in the northern Rocky Mountains of western Montana have been available for decades (Alden, 1932; Carrara, 1987), these records have seldom been used to infer Pleistocene climate (e.g., Murray and Locke, 1989). Many ranges were occupied by coalesced valley glaciers and ice caps with high-altitude ice divides, which are especially difficult to reconstruct based solely on mapped glacial deposits and landforms. Additionally, in much of

https://doi.org/10.5194/cp-2021-106
Preprint. Discussion started: 10 September 2021
© Author(s) 2021. CC BY 4.0 License.

Climate of the Past Discussions

46 northwestern Montana, mountain glaciers likely coalesced with the southern edges of the
47 Laurentide and Cordilleran ice sheets, which also complicates reconstructions of paleo-glaciers,
48 and limits the usefulness of traditional methods for inferring past climate from glacier equilibrium-
49 line altitudes or mass-balance gradients.

50 However, discrete Pleistocene mountain glaciers occupied some ranges of western
51 Montana, as evidenced by a well-preserved record of deposits and landforms delimiting their
52 maximum extent during the last glaciation. Such records are found in the northern Absaroka Range
53 in southwestern Montana and the eastern Lewis Range in northwestern Montana (Figure 1), where
54 glaciers incised deep valleys and in some areas constructed broad terminal moraine complexes
55 along mountain fronts. These records present an opportunity to reconstruct mountain glacier
56 extents and develop cosmogenic chronologies of the last glaciation. These spatiotemporally
57 constrained paleo-glaciers can then, in turn, be used to infer paleoclimate conditions in the northern
58 Rocky Mountains during the last glaciation.

59 Here we present new surficial mapping of latero-terminal moraines of the last Pleistocene
60 glaciation in the Cut Bank and Lake Creek valleys in the eastern Lewis Range and cosmogenic
61 ^{10}Be surface exposure ages of a terminal moraine complex in Cut Bank valley. For the northern
62 Absaroka Range, we present new exposure ages for latero-terminal moraines in South Fork Deep
63 Creek and Cascade Creek valleys as well as glacially scoured bedrock ages from Pine Creek to
64 track ice retreat from a previously dated terminal moraine to a cirque floor. We use the
65 spatiotemporal glacial histories from the Lewis and Absaroka ranges to inform numerical
66 modeling of paleo-glacier shapes, thicknesses and paleoclimate conditions (i.e., precipitation and
67 temperature) for mapped and dated glacial stadials. We then compare the glacial chronologies and
68 glacier-climate modeling results developed for the Lewis and northern Absaroka Ranges to those

https://doi.org/10.5194/cp-2021-106
Preprint. Discussion started: 10 September 2021
© Author(s) 2021. CC BY 4.0 License.

Climate of the Past Discussions
Open Access
EGU

69 from other western North America mountain ranges and examine how these glacial histories can
70 inform our understanding of regional patterns of glaciation and climate change.

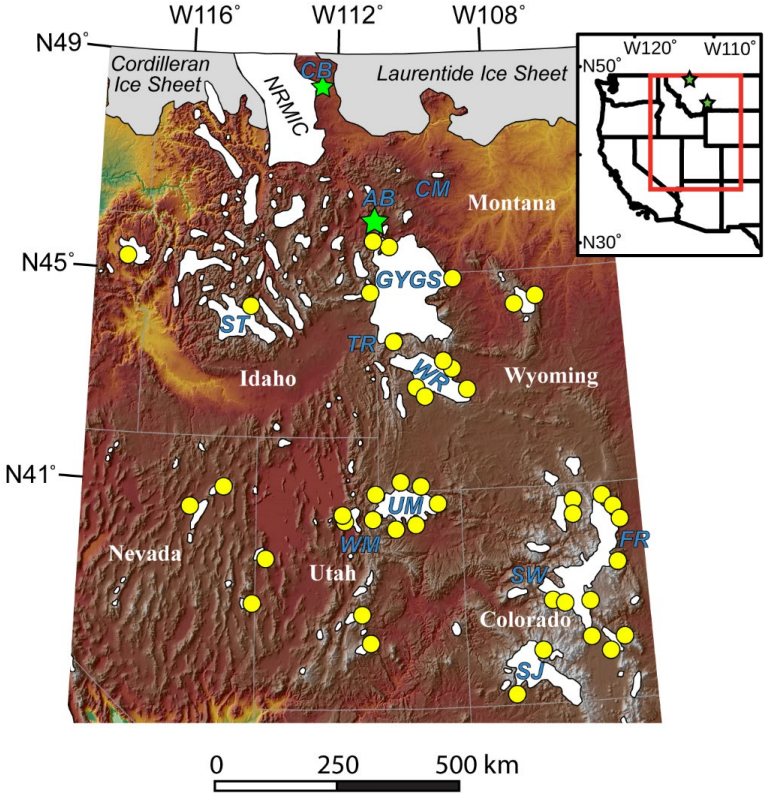

71

72 *Figure 1. Pleistocene ice extents in the northern U.S. Rocky Mountains (after Pierce et al., 1983;*
73 *Pierce, 2003) with the locations of our two field sites, Cut Bank Creek (CB) in the Lewis Range*
74 *and Pine Creek, South Fork Deep Creek, and Cascade Creek in the northern Absaroka Range*
75 *(AB) indicated by green stars. Locations of previously established age control are indicated by*
76 *yellow circles including the Greater Yellowstone glacial system (GYGS), Crazy Mountains (CM),*
77 *Wind River (WR), Sawtooth (ST), Wasatch (WM), Uinta (UM), Front Range (FR), Sawatch (SW),*
78 *and San Juan (SJ) ranges. General outlines of the Cordilleran and Laurentide ice sheets as well*
79 *the northern Rocky Mountain ice cap (NRMIC) are also shown. (Inset) Map of Western North*

https://doi.org/10.5194/cp-2021-106
Preprint. Discussion started: 10 September 2021
© Author(s) 2021. CC BY 4.0 License.

Climate of the Past Discussions

America with state outlines. Green stars indicate our study areas and the red box shows the approximate coverage of the main illustration.

Site Description

The Lewis Range hosted numerous glaciers and, in some areas, coalesced forming the northern Rocky Mountain ice cap (Figure 1). In this study, we focus on the Cut Bank Creek glacier which flowed east from its headwaters at 2.6 km asl and terminated on the piedmont just above 1.4 km asl at its maximum extent. The Cut Bank glacier did not coalesce with either the northern Rocky Mountain ice cap to the west and north or the Laurentide ice sheet to the east during Pinedale times and flowed as a discrete mountain glacier. The glacier was over 25 km long at its maximum extent and in many areas was over 200 meters thick with maximum ice thickness in excess of 300 meters.

The Absaroka Range, located to the north of the Greater Yellowstone glacial system (Figure 1) also hosted several glaciers during Pinedale times including the Pine Creek, South Fork Deep Creek, and Cascade Creek glaciers. The three glaciers flowed from southeast to the northwest just to the range front where they built terminal and lateral moraine complexes. All three canyons have headwaters at or above 3 km asl and generally flowed down to elevations of around 1.6-1.7 km asl. The Pine Creek Pinedale glacier was the longest of the three at over 13 km at it's maximum extent. The Cascade and South Fork Deep Creek glaciers were around 6 and 7 km long at their maximum Pinedale extents, respectively. Ice thicknesses were thinner in the Absaroka Range glaciers as compared to the Cut Bank glacier, with many areas hosting 100-200 meter thick ice and maximum thicknesses in Pine Creek of 250-300 meters.

https://doi.org/10.5194/cp-2021-106
Preprint. Discussion started: 10 September 2021
© Author(s) 2021. CC BY 4.0 License.

Climate of the Past Discussions

Previous Studies

Reconstructions of Pleistocene glaciers in the northern Rocky Mountains of western Montana are limited (Pierce, 2003), and relatively little work has been done inferring past climate in the region from paleoglacier characteristics. Most previous work has focused either on the Greater Yellowstone area of southern Montana or on the Glacier National Park area of northern Montana – also the foci of the current study. In these and other areas of western Montana past workers have identified deposits and landforms from the penultimate and most recent glaciations, generally termed Bull Lake and Pinedale glaciations, following the terminology developed by Blackwelder (1915) for the Wind River Range of Wyoming (Fig. 1). Based on chronologies of glacial deposits throughout the Middle and Southern Rocky Mountains, these last two Pleistocene glaciations are thought to correspond broadly with intervals of global ice volume increase during marine isotope stages (MIS) 2 and 6, respectively (Licciardi and Pierce, 2008; Licciardi and Pierce, 2018; Quirk et al., 2018; Dahms et al. 2018; Schweinsberg et al., 2020; Laabs et al., 2020). Chronological work utilizing cosmogenic nuclide surface-exposure dating in the Yellowstone/Grand Teton National Parks area of southwestern Montana and adjacent northwestern Wyoming (Licciardi et al., 2001; Licciardi and Pierce, 2008, 2018; Pierce et al., 2018) has allowed subdivision of Pinedale-age deposits as is discussed below.

Deposits of Pleistocene mountain glaciers in the eastern Lewis Range of western Montana were mapped and described as early as 1906 by Calhoun and then later by Alden (1932), Carrara (1989), and Fullerton et al. (2004). Calhoun (1906) described the broad hummocky terminal and recessional moraines deposited on the plains to the east of Cut Bank Creek headwaters investigated in this study as well as several recessional moraine ridges deposited up valley. Fullerton et al. (2004) identified multiple Pinedale tills, two ages of Bull Lake till, and a possible pre-Bull Lake

https://doi.org/10.5194/cp-2021-106
Preprint. Discussion started: 10 September 2021
© Author(s) 2021. CC BY 4.0 License.


125 till in moraine deposits at Cut Bank Creek and elsewhere along the eastern front of the Lewis
126 Range. No numerical ages are available for these deposits, although a radiocarbon age on a wood
127 fragment, underlying two latest Pleistocene tephra layers in lake sediment at Marias Pass, provides
128 a minimum age of 12,194±145 ^{14}C yr (Carrara, 1995) or ~14,245 cal yr (Fullerton et al., 2004) for
129 complete recession of at least one east-side outlet glacier of the Northern Montana Ice Cap in the
130 Glacier National Park region.

131 Pleistocene glacial deposits north of Yellowstone National Park and near the northern
132 Absaroka Range were first described and mapped by Weed (1893) and then later by Pierce (1973;
133 1979 and references therein). Licciardi and Pierce (2018) identified three distinct phases of
134 glaciation in the Greater Yellowstone region during the last glacial including the early (22-18 ka),
135 middle (18-16 ka), and late (16-13 ka) Pinedale. While the early Pinedale phase in the Yellowstone
136 area occurred mainly during the interval of the global Last Glacial Maximum (26.5-19.0 ka; Clark
137 et al., 2009); the middle and late Pinedale phases clearly postdated the global LGM, although they
138 appear to have predated the Younger Dryas interval. Terminal and recessional moraines at the
139 southwestern front of the northern Absaroka Range and in the neighboring Paradise Valley to the
140 south of cosmogenic ^{10}Be exposure ages were originally reported by Licciardi et al. (2001) and
141 combined with additional data by Licciardi and Pierce (2008; 2018). The terminal moraine in Pine
142 Creek valley of the northern Absaroka Range has a mean cosmogenic ^{10}Be exposure age of 18.2
143 ± 0.5 ka (± 1 standard error of the mean) as recalculated using methods described in the text. In
144 Paradise Valley, moraines delimiting the terminus of the northern outlet of the Yellowstone glacial
145 system have mean 10Be exposure ages of 17.9 ± 0.4 ka for the Eightmile terminal moraine and
146 17.1 ± 0.6 ka for the Chico recessional moraine. Together, these exposure ages indicate that
147 mountain glaciers in this sector of the Greater Yellowstone glacial system began retreating from

https://doi.org/10.5194/cp-2021-106
Preprint. Discussion started: 10 September 2021
© Author(s) 2021. CC BY 4.0 License.


148 their terminal moraines during the middle Pinedale and, critically, after the end of the global Last
149 Glacial Maximum.

150 Less attention has been paid by previous workers to use of paleoglaciological methods to
151 reconstruct late Pleistocene climate in western Montana than to reconstruction of the extent and
152 chronology of past glaciation. Locke (1990) examined modern and reconstructed late Pleistocene
153 glacier equilibrium lines throughout western Montana, concluding that an assumed late Pleistocene
154 temperature depression of 10°C would have been associated with decreased precipitation relative
155 to the present. Based on mapping of glacial deposits and landforms in the Crazy Mountains of
156 southwestern Montana (Figure 1), Murray and Locke (1989) reconstructed the geometry and ice
157 flux of a valley glacier in Big Timber Canyon. They interpret the reconstructed ice-surface gradient
158 and ice flux as indicators of a cold and dry regional climate during the last glaciation. Hostetler &
159 Clark (1997) used a combination of climate-model output and glacier equilibrium-line modeling
160 and concluded that during the LGM in the Yellowstone region summer temperatures were 10-
161 15°C colder than present with winter precipitation approximately equal to present, while in
162 northern Montana winter temperature depression was even greater but precipitation was reduced
163 compared to modern.

164 Nowhere in the U.S. northern Rocky Mountains have more recent
165 paleoglaciological methods, particularly distributed energy/mass-balance models or degree-day
166 mass-balance models, been applied to reconstructed late Pleistocene glaciers, as they have been
167 successfully applied in the Middle Rocky Mountains (Laabs et al., 2006; Refsnider et al., 2008;
168 Birkel et al., 2012; Quirk et al., 2018, 2020) and Southern Rocky Mountains (Ward et al., 2009;
169 Brugger, 2010; Brugger et al. 2018, 2019; Dühnforth and Anderson, 2011; Leonard et al., 2014,
170 2017a; Schweinsberg et al., 2016;). In this study we apply a modified version of the Plummer and

https://doi.org/10.5194/cp-2021-106
Preprint. Discussion started: 10 September 2021
© Author(s) 2021. CC BY 4.0 License.

Climate of the Past Discussions

171 Phillips (2003) distributed energy/mass-balance model to reconstructed glaciers in the Absaroka
172 and Lewis ranges to help elucidate climate conditions in the northern Rockies during the last
173 glaciation.
174 .

175 **METHODS**

176 **Moraine Mapping**

177 Although terminal moraines of east-flowing glaciers in the Lewis Range are known from
178 previous studies, they were remapped here to aid with reconstructing maximum ice extent in the
179 Cut Bank Creek and Lake Creek valleys (Figure 2a). Moraines in both valleys were examined in
180 aerial imagery available in Google Earth and using 1:24,000-scale topographic maps. The portion
181 of the terminal moraine north of Cut Bank Creek was mapped in the field. Moraines were identified
182 as broad (0.5-1 km wide), looping plateaus with hummocky topography (Figure 3) on the piedmont
183 east of the Lewis Range and featured abundant erratic boulders at their crests.

184 Surficial mapping of glacial deposits within our area of interest in the Absaroka Range had
185 been previously completed by Pierce (1979 and references therein). Mapping in the Pine Creek
186 area was subsequently updated by Licciardi and Pierce (2008). In the field, we checked and
187 confirmed, without modification, the moraine mapping from these previous studies.

https://doi.org/10.5194/cp-2021-106
Preprint. Discussion started: 10 September 2021
© Author(s) 2021. CC BY 4.0 License.

Climate of the Past
Discussions
Open Access
EGU

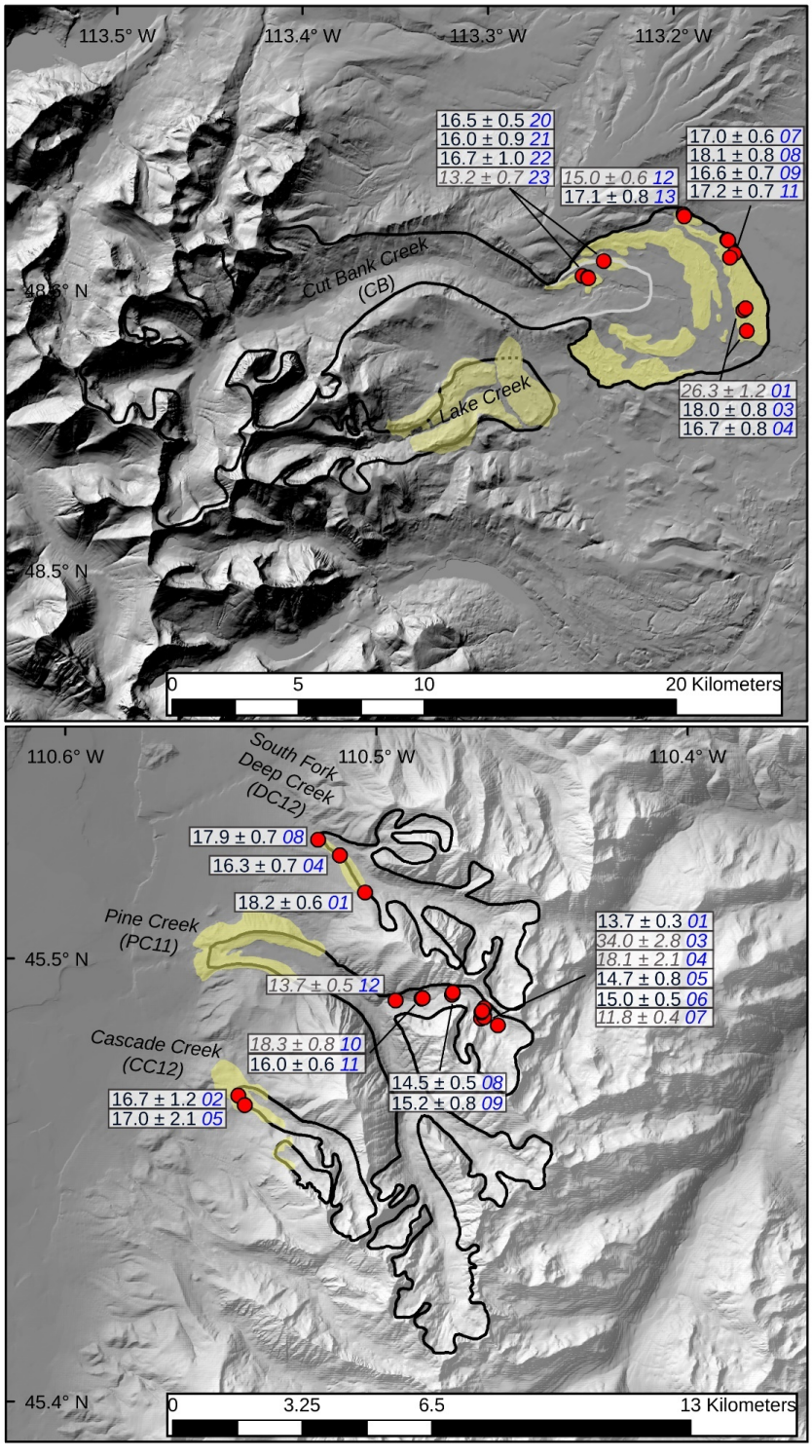

https://doi.org/10.5194/cp-2021-106
Preprint. Discussion started: 10 September 2021
© Author(s) 2021. CC BY 4.0 License.

Climate of the Past Discussions
Open Access
EGU

189 *Figure 2. (Top) Cut Bank Creek study area located in the Lewis Range of northern Montana.*
190 *(Bottom) northern Absaroka Range study area including South Fork Deep Creek, Pine Creek, and*
191 *Cascade Creek drainages. Pinedale maximum ice extents are outlined in black (dashed where*
192 *inferred). Recessional position at Cut Bank outlined in light-grey. Moraine deposits are shown in*
193 *yellow with cosmogenic ^{10}Be boulder sample locations indicated by the red circles with exposure*
194 *ages and analytical uncertainty (shown in ka) and sample codes in blue text. Exposure ages*
195 *interpreted as outliers are shown in grey and italicized.*

https://doi.org/10.5194/cp-2021-106
Preprint. Discussion started: 10 September 2021
© Author(s) 2021. CC BY 4.0 License.

Figure 3. (A) Characteristic hummocky morphology of Cut Bank Creek terminal moraine. (B) Boulder CB-03 targeted for cosmogenic exposure dating on the Cut Bank terminal moraine. (C) Photograph taken facing north-northeast looking across the threshold of Pine Creek Lake and towards bedrock sampled for cosmogenic exposure dating. (D) Location of bedrock sample PC11-

https://doi.org/10.5194/cp-2021-106
Preprint. Discussion started: 10 September 2021
© Author(s) 2021. CC BY 4.0 License.

Climate of the Past Discussions

11. (E) Lateral sector of the Cascade Canyon Pinedale terminal moraine. (F) South Fork Deep Creek lateral moraine sample DC12-01.

Cosmogenic ^{10}Be Exposure Dating

Following moraine mapping and field verification, we selected moraines and erratic boulders atop moraine crests for *in-situ* cosmogenic ^{10}Be exposure dating to determine landform ages. at Cut Bank Creek, South Fork Deep Creek, and Cascade Creek canyons. Boulders atop a recessional moraine identified just beyond the mouth of Cut Bank Canyon were also sampled to limit the time when moraine building at the mountain front ceased and ice retreat commenced.

On moraine crests, we searched for large (>0.5 m tall), quartz-bearing boulders with broad horizontal surfaces. When possible, we selected boulders and bedrock surfaces with clear glacial polish and/or striations. In the northern Absaroka Range, most sampled moraine-boulders consisted of Jewel Quartzite (Archean rocks of the Wyoming Province; Zientek et al., 2005), which generally contains >90% quartz and some accessory minerals. In the Cut Bank Creek valley, sampled moraine boulders consisted of silica-cemented quartz arenite derived from the Appekunny Formation (subdivided from the Proterozoic Belt Supergroup), which is widely exposed along bedrock divides in the Lewis Range (Whipple et al., 1984). By selecting only samples with clear glacial polish and/or striations we determined that sample surface erosion was insignificant, and we therefore used an erosion rate of 0 cm a^{-1} in exposure age calculations. Samples were collected using a hammer and chisel to depths ranging from 1 – 5 cm, with an average depth of 3 cm. The number of samples collected from each landform varied based on the availability of suitable targets. Topographic shielding data were collected in the field with a clinometer. Target surfaces were selected so as to minimize the effect of internal shielding and cosmic ray scattering from nearby boulders.

https://doi.org/10.5194/cp-2021-106
Preprint. Discussion started: 10 September 2021
© Author(s) 2021. CC BY 4.0 License.

Climate of the Past Discussions

224 At Pine Creek in the northern Absaroka Range, where cosmogenic ^{10}Be exposure ages of
225 latero-terminal moraines were already available (Licciardi and Pierce, 2008), glacially scoured
226 bedrock and erratic boulders were sampled along the path of ice retreat. Here, we assume that
227 bedrock surfaces became progressively exposed through time as ice retreated up valley from the
228 terminal moraine and, therefore, exposure ages would limit the pace and timing of ice retreat (cf.
229 Guido et al., 2007). Jewel Quartzite, described above, bedrock and erratic boulders were sampled
230 along the length of the transect and were collected following the same procedure described above.
231 All samples were prepared at SUNY Geneseo for in-situ cosmogenic ^{10}Be measurement
232 following methods in Laabs et al. (2013). Samples were crushed, milled, and sieved to a target
233 grain size of 250-500 μm. Quartz grains were isolated using a rare earth hand magnet, Franz
234 magnetic separator, density separation, and dilute acid treatment. The quartz purification process
235 was accomplished by repeated etching in dilute hydrofluoric and nitric acids (Kohl and Nishiizumi,
236 1992). Prior to dissolution in concentrated hydrofluoric acid, the purified quartz fraction of each
237 sample was spiked with a commercially made ^{9}Be carrier solution purchased from SPEX CertiPrep
238 with a certified Be concentration of 1 mg/mL. Procedural blanks were prepared using equal carrier
239 mass as was added to samples. The beryllium fraction of each sample was chemically isolated and
240 loaded into targets for ^{10}Be/^{9}Be measurement by accelerator mass spectrometry (AMS) at the
241 Purdue University Rare Isotope Measurement Laboratory (Sharma et al., 2000; Muzikar et al.,
242 2003). All ^{10}Be/^{9}Be values were normalized to the AMS beryllium standard 07KNSTD
243 (Nishiizumi et al., 2007).
244 We calculated cosmogenic ^{10}Be exposure ages using the Balco et al. (2008) online
245 exposure age calculator, version 3.0 (http://hess.ess.washington.edu/math/). This calculator and
246 version were selected because they implement the Lifton-Sato-Dunai nuclide dependent (LSDn;

https://doi.org/10.5194/cp-2021-106
Preprint. Discussion started: 10 September 2021
© Author(s) 2021. CC BY 4.0 License.

Climate of the Past Discussions

247 Lifton et al., 2014) scaling model and production rates based on user-defined calibration data from
248 independently dated locations. Production rates were computed using *in situ* ^{10}Be data from the
249 independently dated surface at the Promontory Point production-rate calibration site reported by
250 Lifton et al. (2015), which features well-preserved and continuously exposed surfaces following
251 the Bonneville Flood at 18,350 ± 300 cal. yr BP. We chose this calibration site because of its
252 proximity in space and time to the study area, following other recent reports of Pleistocene moraine
253 chronologies in the Rocky Mountains (Licciardi and Pierce, 2018; Schweinsberg et al., 2020;
254 Laabs et al., 2020). Moraine ages and associated uncertainties are reported as the arithmetic mean
255 of individual boulder exposure ages and the standard error of the mean, respectively (as in Putnam
256 et al., 2010; Quirk et al., 2020).

257 **Glacier Modeling**

258 The coupled energy/mass-balance and ice-flow models used in this study were originally
259 developed by Plummer and Phillips (2003) and have been successfully used to estimate
260 paleoclimate conditions for extinct glaciers in a variety of geologic settings (Quirk et al., 2020;
261 Rowan et al., 2014; Leonard et al., 2014; Harrison et al., 2014; Laabs et al., 2006). Additionally,
262 several studies have verified the model's ability to successfully predict snow accumulation (Laabs
263 et al., 2006; Leonard et al., 2014) and melt (Quirk et al., 2020), as well as small glacier extents
264 (Plummer, 2002) for modern conditions in the western U.S.

265 Our modeling approach is to match simulated glacier extents produced under prescribed
266 climate perturbations relative to modern (e.g., temperature depression and precipitation change) to
267 field evidence such as terminal and lateral moraines. In this study, we match modeled glacier
268 shapes and thicknesses to the well-defined Pinedale maximum ice extents at Cut Bank, Pine Creek
269 and South Fork Deep Creek. In order to test the validity of the ice flow parameters used for the

https://doi.org/10.5194/cp-2021-106
Preprint. Discussion started: 10 September 2021
© Author(s) 2021. CC BY 4.0 License.


Cut Bank Creek glacier detailed below, we reconstructed the undated Lake Creek glacier immediately to south of Cut Bank at its maximum mapped extent using the same parameters. We reconstructed the Cut Bank glacier using a model spatial resolution of 180 m while we used a resolution of 30 m for the Pine Creek and South Fork Deep Creek glaciers, which were modeled in the same domain (herein the northern Absaroka domain). We did not include Cascade Creek as a target for glacier reconstructions because mapping of the glacier's exact terminal position remains unresolved.

The energy/mass-balance model calculates snow accumulation and ablation at every cell within the model domain for the time interval of interest, typically one to several years. Annual mass balance depends mostly on precipitation and temperature, which are the principal inputs to the model. In this study, we use a similar approach to the one used by Leonard et al. (2017a) whereby we describe the monthly spatial distribution of temperature and precipitation at every cell across the model domain with linear regressions of elevation and PRISM (Parameter-elevation Regression on Independent Slopes Model http://www.prism.oregonstate.edu/; Daly et al., 2008) monthly mean climatological models. Secondary climate parameters include estimates of average monthly relative humidity, cloudiness, and wind speed, and are taken directly or derived from a combination of RAWS and NOAA COOP Station historical weather station data. We calculated average monthly cloudiness for the Cut Bank and Lake Creek Canyon domains by determining the fraction of days per month with precipitation (i.e. 0.5 cloudiness = 15 days of precipitation / 30 days total). For the Pine and South Fork Deep Creek domain, cloudiness was estimated using the ERA-Interim 3rd generation (1979-2015) reanalysis (http://cci-reanalyzer.org/reanalysis/monthly_tseries/). Wind speed (Ws) was scaled for elevation from

https://doi.org/10.5194/cp-2021-106
Preprint. Discussion started: 10 September 2021
© Author(s) 2021. CC BY 4.0 License.

Climate of the Past Discussions

292 weather station data using a given weather station's reference elevation (Elevation $_{REF}$) using the
293 equation:

294 (1) $W_s = W_{SREF} + (Elevation - Elevation_{REF}) * k$

295 where W_{SREF} is wind speed at the reference elevation and k is a wind scaling factor. Here, k is
296 taken as 0.001, resulting in an additional 1 m s^{-1} average wind speed per 1000 m elevation. Average
297 monthly cloudiness is held constant at every cell and elevation within the model domain. To
298 simulate paleo-glacier extents, we varied precipitation and temperature, the two dominant climate
299 input parameters, using multiplicative and additive variations from modern, respectively. Thus, a
300 precipitation factor change of 1 is equal to modern precipitation and a temperature of depression
301 of 0 °C is modern temperature.

302 The primary output from the energy/mass-balance model is a mass-balance grid for model
303 domain. The mass-balance grid is input to the ice-flow model along with a digital elevation model
304 of the drainage basins. The ice-flow model designed by Plummer and Phillips (2003) used here is
305 similar to the finite-element ice sheet model described by Fastook and Chapman (1989) and
306 follows the commonly used shallow-ice approximation. Snow and ice mass is gained in the
307 accumulation zone and flows along the ice-surface gradient via deformation and sliding into the
308 ablation zone. We run glacier simulations to steady-state where the simulated terminus stabilizes
309 at a mapped moraine position. We define steady-state condition in our model runs as when the
310 integrated surface balance errors are less than 5%, and typically ≈ 0%, as described by Plummer
311 and Phillips (2003). The time-dependent ice-flow model is an alternating direction-implicit, space
312 -entered, finite-difference form of the continuity equation for 2-D flow:

313 (2) $\partial h/\partial t = b_n - \partial q_x/\partial x - \partial q_y/\partial y$

https://doi.org/10.5194/cp-2021-106
Preprint. Discussion started: 10 September 2021
© Author(s) 2021. CC BY 4.0 License.

Climate of the Past Discussions

where h = ice-surface elevation, b_n = net annual mass balance, q = ice discharge per unit width, and x and y are orthogonal directions of ice flow in the horizontal plane. The ice flux between neighboring cells is determined by the thickness and depth-integrated flow velocity, U, which is the sum of ice flow via deformation and sliding:

$$U = u_d + u_s = (1\text{-}f)\, H\, 2/5\, (\tau A)^m + f\, (\tau B)^n \quad (3)$$

Here A is the deformation flow coefficient, B is the sliding flow coefficient, H is ice thickness, f is a velocity scaling parameter, and τ is basal shear stress. The exponents m and n are taken to be 3 and 2, respectively, as described by Fastook and Chapman (1989). We tuned ice flow parameters A, B, and f to match simulated glacier shapes and ice thicknesses to the observational record. Ice flow parameter values that simulated observed ice thicknesses well included A values for the Cut Bank and northern Absaroka domains of 8.0 E-5 a^{-1} kPa^{-3} and 1.0 E-7 a^{-1} kPa^{-3}, and B values of 0.0015 m a^{-1} kPa^{-2}, and f values of 0 and 0.5, respectively. The ice-flow parameters used in northern Absaroka domain agree well with the published range of values used in previous glacier flow models (Oerlemans, 1989; Plummer and Phillips, 2003; Laabs et al., 2006; Quirk et al., 2018).

The Cut Bank glacier required a greater value of the deformation flow coefficient compared to the steeper valley glaciers in the northern Absaroka Range. Although it is likely that the Cut Bank Creek glacier was sliding at its base, we did not account for the contribution of sliding to flow because it was likely far less than the contribution to flow by deformation as indicated by the great ice thicknesses and low surface slopes. As described previously, we also simulated the Lake Creek glacier immediately south of Cut Bank using identical ice-flow parameters to test the validity of the chosen values. Through experimentation, we tuned the ice-flow parameters to produce simulated steady-state glaciers that matched the mapped paleo-glacier thickness and shape

https://doi.org/10.5194/cp-2021-106
Preprint. Discussion started: 10 September 2021
© Author(s) 2021. CC BY 4.0 License.


in both valleys and thus parameterized the effects the piedmont lobe and glacier shape had on the Cut Bank glacier. (Supplemental Figure 1).

RESULTS

Moraine Mapping

The suite of moraines deposited at the mountain front in Cut Bank Creek valley features three broad, looping plateaus with hummocky topography separated by incised meltwater channels and outwash. The suite includes a multi-crested terminal moraine deposited farthest beyond the mountain front and a recessional moraine deposited near the mouth of Cut Bank Canyon (Figure 2). The ice-distal sector of the terminal moraine has the highest internal relief (up to 30 m) along the portion of the moraine south of Cut Bank Creek, with numerous closed depressions, some of which are filled with shallow lakes. The distal slope of the moraine grades to a broad, gently sloping outwash plain known locally as Starr School Flat, featuring low-relief (<3 m) depressions and abandoned braided channels. The ice-proximal sector of the terminal moraine is narrower with less internal relief (less than 15 m) and fewer closed depressions. The proximal slope of this sector of the moraine appears to be partially buried by outwash where it is bisected by Cut Bank Creek. The recessional moraine is best preserved north of Cut Bank Creek and features low-relief hummocky topography (less than 5 m internally). In Lake Creek valley, only a single, looping terminal-moraine ridge is preserved at the mountain front, forming a broad area of hummocky topography with greater internal relief (up to 60 m along portions north Lake Creek).

The moraines delimit the size and shape of the piedmont lobes formed by glaciers in the two valleys. In Cut Bank Creek valley, the piedmont lobe had a maximum diameter of 6.8 km while occupying the distal sector of the moraine. While occupying the ice-proximal sector, the piedmont lobe was reduced in diameter to approximately 4.4 km and likely became thinner or

https://doi.org/10.5194/cp-2021-106
Preprint. Discussion started: 10 September 2021
© Author(s) 2021. CC BY 4.0 License.

Climate of the Past Discussions

359 formed a more gradual slope near the terminus as evidenced by the lower relief along the moraine.
360 The piedmont glacier width was further diminished upon retreat to the recessional moraine to
361 approximately 1.3 km, only slightly wider than the mouth of Cut Bank Canyon. In Lake Creek
362 valley, the piedmont lobe formed an irregular shape, likely due to partial confinement of the
363 northern side of the lobe by the right-lateral moraine in the neighboring Cut Bank Creek valley.
364 The piedmont lobe had a maximum width of about 2.5 km when the terminal moraine was
365 occupied. Upvalley of the terminal moraines in Cut Bank Creek and Lake Creek valleys, lateral
366 moraines and other glacial features mapped by Carrara (1989) were used to delimit ice thickness
367 and areal extent.

368 **Cosmogenic ^{10}Be Exposure Ages**

369 Here we present 29 cosmogenic ^{10}Be exposure ages collected from glaciated catchments
370 in the Lewis and northern Absaroka Ranges of Montana (Figure 2; Figure 4). In the Lewis Range,
371 nine exposure ages are from the ice-distal sector of the terminal moraine in Cut Bank Creek valley
372 and four are from a recessional moraine up valley. In the northern Absaroka Range, two samples
373 are from the Cascade Creek lateral moraine, three are from the South Fork Deep Creek lateral
374 moraine, and eleven are Pine Creek Canyon bedrock and erratic samples. The ^{10}Be/^{9}Be ratios in
375 procedural blanks ranged from 6.00×10^{-15} to 4.90×10^{-14}. Sample ^{10}Be/^{9}Be ratios ranged from
376 3.18×10^{-13} to 1.37×10^{-12} (Supplemental Table 1). The range of AMS measurement uncertainties
377 (one sigma) for most samples was approximately 1.5 – 3.5%. Both moraine-boulder samples from
378 Cascade Creek have greater AMS errors of 4.9% (CC12-02) and 8.3% (CC12-05).

379 We identified three outliers among moraine exposure ages, including samples CB-01,
380 CB-12 from the Cut Bank terminal and CB-23 from the Cut Bank recessional moraine (Table 1).
381 Sample CB-01 is more than 8 ka older than all other boulder exposure ages from the terminal

https://doi.org/10.5194/cp-2021-106
Preprint. Discussion started: 10 September 2021
© Author(s) 2021. CC BY 4.0 License.

382 moraine and is therefore interpreted to reflect inherited ^{10}Be nuclide inventory in the surface from
383 a period of prior exposure. Sample CB-12 is younger than all but one of the exposure ages on the
384 upvalley recessional moraine, which is interpreted to represent incomplete or inconsistent
385 exposure history since the terminal moraine was deposited. Sample CB-23 has an exposure age 3
386 ka younger than the three other boulders from the moraine and is also interpreted to represent
387 incomplete or inconsistent exposure history since the recessional moraine was deposited. Although
388 we found no evidence in the field for inconsistent exposure histories among the sampled boulders,
389 these young exposure ages could be explained by several geologic processes including local burial
390 by sediment followed by exhumation, or significant boulder-surface erosion rates. The mean of
391 the remaining seven ^{10}Be exposure ages from the terminal moraine in Cut Bank Creek valley limit
392 its abandonment to 17.2 ± 0.2 ka. The abandonment age of the recessional moraine, 16.4 ± 0.2 ka,
393 is defined by three exposure ages.

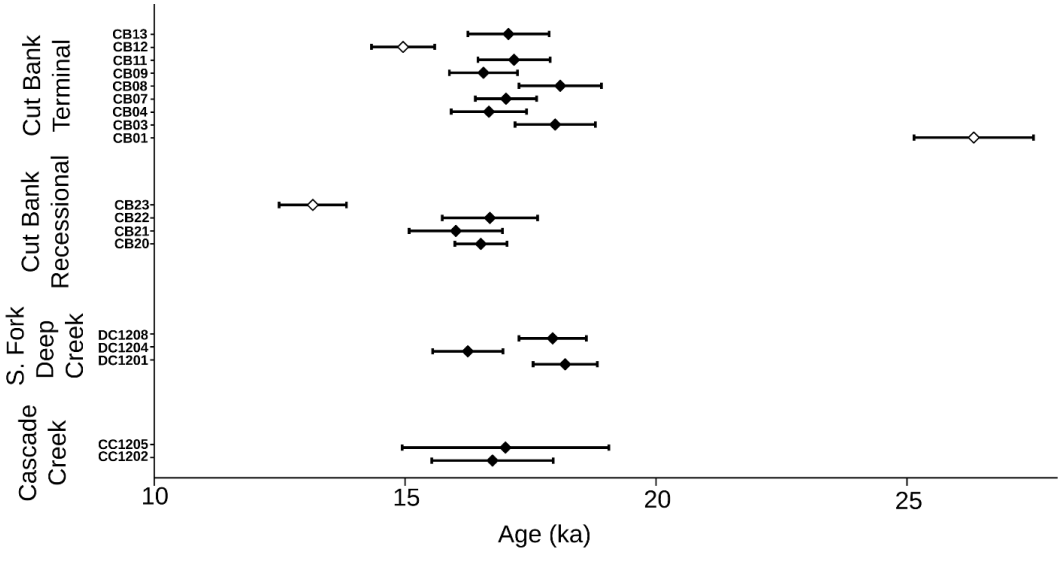

394

395 *Figure 4. Cosmogenic ^{10}Be exposure ages with analytical uncertainties for samples collected from*
396 *moraines at Cascade Creek and South Fork Deep Creek in the Absaroka Range and moraines at*

https://doi.org/10.5194/cp-2021-106
Preprint. Discussion started: 10 September 2021
© Author(s) 2021. CC BY 4.0 License.

Climate of the Past Discussions

Cut Bank in the Lewis Range. Samples that have been identified as outliers are denoted by open symbols.

Abandonment ages for the two moraines in the northern Absaroka Range at Cascade Canyon and South Fork Deep Creek are limited by the means of two and three boulder exposure ages at 16.9 ± 0.1 ka and 17.5 ± 0.6 ka, respectively, although we reiterate that the exposure ages of the lateral moraine at Cascade Canyon are considered preliminary because of the greater-than-expected AMS measurement errors.

The set of bedrock exposure ages from the ice-recessional path in Pine Creek valley includes one (PC11-03, 34.0 ± 2.8 ka) that exceeds the exposure age of the lateral moraine downvalley (18.2 ± 0.5 ka, Licciardi and Pierce, 2008) and two (PC11-04 and PC11-10, 18.1 ± 2.1 and 18.3 ± 0.8 ka, respectively) that overlap with it. These surfaces are interpreted to reflect inherited ^{10}Be from a period of prior exposure, which suggests that glacial scouring during the last glaciation at these sample sites was insufficient to remove the ^{10}Be inherited from pre-glacial exposure of the valley floor. Two samples, PC11-07 and PC11-12, yield exposure ages younger than surfaces sampled at upvalley positions and are interpreted to reflect incomplete exposure due to burial by sediment. Sample PC11-07 is from an erratic boulder atop a bedrock surface with exposure ages 3 kyr older, suggesting that the boulder, originally interpreted to be an erratic deposited by glacier ice during recession, has been reworked by fluvial and mass-movement processes. The remaining six exposure ages range from 16.0 ± 0.6 ka at the farthest downvalley site (PC11-11) to 13.7 ± 0.3 ka at the farthest up valley site (PC11-01) in the cirque occupied by Pine Creek Lake. When combined with the mean exposure age of the latero-terminal moraine of 18.2 ± 0.5 ka, these exposure ages record the pace and timing of ice retreat over a period of ~4 kyr.

https://doi.org/10.5194/cp-2021-106
Preprint. Discussion started: 10 September 2021
© Author(s) 2021. CC BY 4.0 License.

Climate of the Past Discussions
Open Access
EGU

Table 1. Cosmogenic ^{10}Be sample information and exposure ages

Sample ID	Latitude	Longitude	Elevation (m)	Thickness (cm)	Density (g cm^{-2})	Shielding Factor	Erosion rate (cm yr^{-1})	[Be-10] (atmos g^{-1})	+/-	Exposure Age (ka)	Analytical Error (ka)	External Error (ka)
Cut Bank Terminal Moraine												
CB-01	48.5936	-113.1555	1444	1	2.65	1	0	3.96E+05	1.78E+04	26.3	1.2	1.6
CB-03	48.6009	-113.1577	1452	3	2.65	1	0	2.64E+05	1.17E+04	18.0	0.8	1.1
CB-04	48.6016	-113.1565	1450	3.8	2.65	1	0	2.42E+05	1.08E+04	16.7	0.8	1.0
CB-07	48.6260	-113.1673	1474	4.3	2.65	1	0	2.51E+05	8.93E+03	17.0	0.6	0.9
CB-08	48.6257	-113.1670	1472	3	2.65	1	0	2.70E+05	1.21E+04	18.1	0.8	1.1
CB-09	48.6210	-113.1633	1465	3	2.65	1	0	2.45E+05	1.00E+04	16.6	0.7	0.9
CB-11	48.6196	-113.1656	1469	3	2.65	1	0	2.55E+05	1.07E+04	17.2	0.7	1.0
CB-12	48.6345	-113.1913	1523	3	2.65	1	0	2.31E+05	9.61E+03	15.0	0.6	0.8
CB-13	48.6338	-113.1910	1518	2.8	2.65	1	0	2.64E+05	1.25E+04	17.1	0.8	1.0
								Landform Age (ka)		**17.2**		
								Standard Error (ka)		**0.2**		
Cut Bank Recessional Moraine												
CB-20	48.6170	-113.2336	1539	4	2.65	1	0	2.57E+05	8.07E+03	16.5	0.5	0.8
CB-21	48.6115	-113.2447	1544	4	2.65	1	0	2.50E+05	1.44E+04	16.0	0.9	1.1
CB-22	48.6111	-113.2418	1534	2	2.65	1	0	2.63E+05	1.49E+04	16.7	1.0	1.1
CB-23	48.6108	-113.2414	1532	5	2.65	1	0	2.01E+05	1.02E+04	13.2	0.7	0.8
								Landform Age (ka)		**16.4**		
								Standard Error (ka)		**0.2**		
Cascade Creek												
CC12-02	45.4688	-110.5449	1934	4	2.65	0.995	0	3.31E+05	2.39E+04	16.7	1.2	1.4
CC12-05	45.4666	-110.5428	1968	4	2.65	0.995	0	3.45E+05	4.17E+04	17.0	2.1	2.2
								Landform Age (ka)		**16.9**		
								Standard Error (ka)		**0.1**		
S. Fork Deep Creek Lateral Moraine												
DC12-01	45.5145	-110.5039	2093	4	2.65	0.989	0	4.05E+05	1.41E+04	18.2	0.6	0.9
DC12-04	45.5229	-110.5120	1927	4	2.65	0.993	0	3.19E+05	1.37E+04	16.3	0.7	0.9
DC12-08	45.5264	-110.5192	1815	3	2.65	0.994	0	3.28E+05	1.22E+04	17.9	0.7	1.0
								Landform Age (ka)		**17.5**		
								Standard Error (ka)		**0.6**		
Pine Creek Bedrock and Erratic												
PC11-01	45.4840	-110.4626	2761	2	2.65	0.975	0	4.84E+05	1.17E+04	13.7	0.3	0.6
PC11-03	45.4859	-110.4668	2774	3	2.65	0.314	0	4.08E+05	3.38E+04	34.0	2.8	3.1
PC11-04	45.4862	-110.4664	2768	2	2.65	0.978	0	6.55E+05	7.56E+04	18.1	2.1	2.2
PC11-05	45.4885	-110.4667	2752	2	2.65	0.955	0	5.09E+05	2.59E+04	14.7	0.8	0.9
PC11-06	45.4885	-110.4670	2757	3	2.65	0.959	0	5.18E+05	1.74E+04	15.0	0.5	0.8
PC11-07	45.4886	-110.4668	2765	2.5	2.65	0.956	0	4.21E+05	1.47E+04	11.8	0.4	0.6
PC11-08	45.4919	-110.4772	2509	3	2.65	0.918	0	4.03E+05	1.40E+04	14.5	0.5	0.7
PC11-09	45.4919	-110.4773	2508	3	2.65	0.918	0	4.23E+05	2.25E+04	15.2	0.8	1.0
PC11-10	45.4912	-110.4873	2262	2.3	2.65	0.947	0	4.48E+05	2.02E+04	18.3	0.8	1.1
PC11-11	45.4914	-110.4870	2276	3	2.65	0.940	0	3.88E+05	1.33E+04	16.0	0.6	0.8
PC11-12	45.4898	-110.4939	2110	3	2.65	0.952	0	2.95E+05	1.03E+04	13.7	0.5	0.7

Underlined indicates outlier samples

Glacier Climate Reconstructions

Model simulations were completed for the Cut Bank and northern Absaroka model domains including four simulations matching the: Cut Bank terminal moraine (CB_T), Cut Bank recessional moraine (CB_R), and Pine Creek and South Fork Deep Creek lateral sectors of terminal moraines (NA_T; Figure 5). For simplicity, each of the sets of four simulations pin precipitation

https://doi.org/10.5194/cp-2021-106
Preprint. Discussion started: 10 September 2021
© Author(s) 2021. CC BY 4.0 License.

Climate of the Past Discussions

425 change (P_x) to multiplicative factors of 0.5, 1.0, 2.0, and 3.0 times modern precipitation, while
426 temperature depressions (T_d) were independently varied in each experiment to match mapped ice
427 extents. In each of the 12 experiments, calculated ice extents and thicknesses matched well with
428 field evidence. The twelve experiments define 3 curves (Figure 6), in T_d-P_x space, representing
429 paleoclimate estimates for ice matching CB_T ($R^2 = 0.98$), CB_R ($R^2 = 0.99$) NA_T ($R^2 = 0.99$) with
430 equations:

431 (4) CB_T $P_x = 24.084e^{0.3589Td}$

432 (5) CB_R $P_x = 6.3721e^{0.2417Td}$

433 (6) NA_T $P_x = 16.877e^{0.3379Td}$

https://doi.org/10.5194/cp-2021-106
Preprint. Discussion started: 10 September 2021
© Author(s) 2021. CC BY 4.0 License.

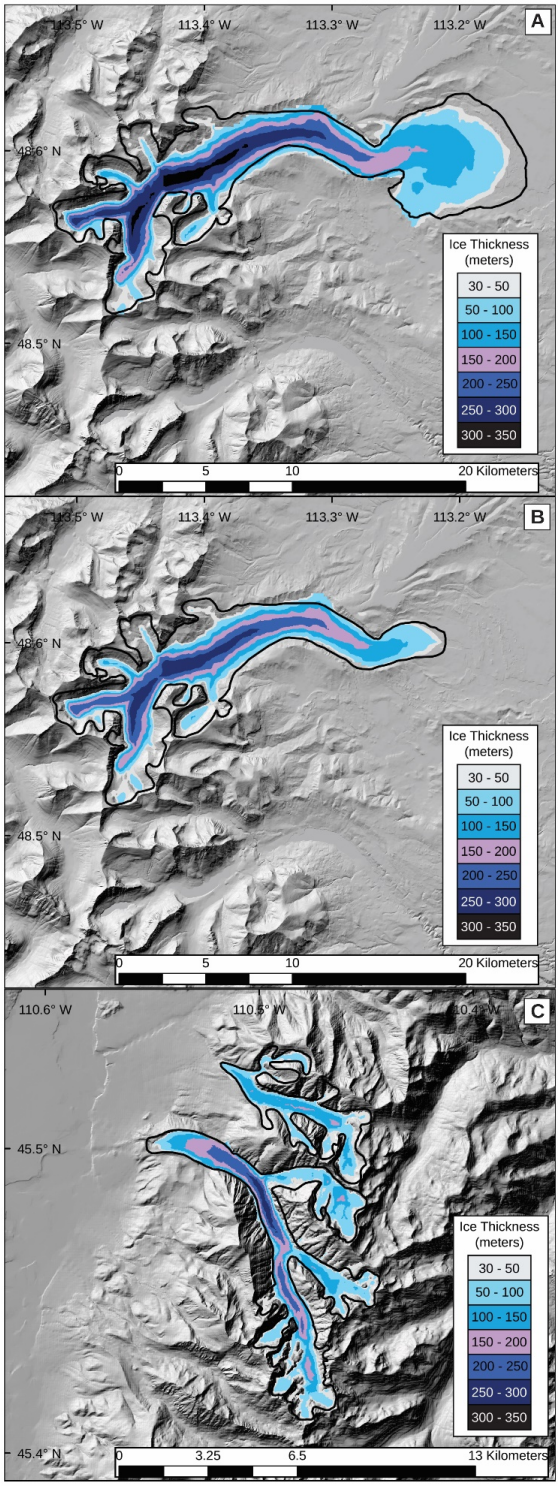

Figure 5. Ice thickness maps generated

https://doi.org/10.5194/cp-2021-106
Preprint. Discussion started: 10 September 2021
© Author(s) 2021. CC BY 4.0 License.

Climate of the Past Discussions

435 *from coupled energy-mass balance and ice-flow modeling for A) Cut Bank terminal B) Cut Bank*
436 *recessional and C) Pine Creek and South Fork Deep Creek in the Absaroka Range. Modeled ice-*
437 *extents were matched to field evidence (black outlines) by varying precipitation (P_x) and*
438 *temperature (T_d) by multiplicative and additive changes, respectively. For each simulation, we*
439 *found a series of P_x-T_d combinations that produced modeled ice extents that satisfactorily matched*
440 *field evidence.Ice extents shown here use 100% modern precipitation and temperature depressions*
441 *of -9.2, -8.0, and -8.5 for the Cut Bank terminal (A), Cut Bank recessional (B), and Absaroka*
442 *Range model domains, respectively.*

443 As previously mentioned, in order to match the modeled glacier shape to field evidence at Cut
444 Bank, we found it necessary to effectively set the contribution of ice velocity due to sliding to zero.
445 In order to test how realistic these model conditions were for reconstructing other glaciers, we
446 reconstructed the Pinedale glacier that occupied Lake Creek Canyon, the drainage immediately to
447 the south of Cut Bank. We matched the modeled glacier to the mapped Pinedale maximum in Lake
448 Creek Canyon with T_d-P_x combinations of -8°C & 100% and -6°C & 190% (Supplemental Figure
449 1). These T_d-P_x combinations are both approximately 1°C warmer than results for Cut Bank's
450 Pinedale maximum glacier given then same precipitation change. However, we find this
451 compelling evidence that the ice flow parameters we used to reconstruct the Cut Bank Pinedale
452 glacier are reasonable. The temperature discrepancy between the two sites could be 1) a result
453 temporal offset between the two maxima as we do not have a landform age for the Lake Creek
454 terminal moraine 2) a real climatic difference between the two catchments and/or 3) a reflection
455 of unaccounted for modeling error. With regards to the latter, we assume model uncertainties
456 matching those reported in Quirk et al. (2020) of ± 1.0°C and 30% for temperature and

https://doi.org/10.5194/cp-2021-106
Preprint. Discussion started: 10 September 2021
© Author(s) 2021. CC BY 4.0 License.


457 precipitation respectively – which indicate overall agreement between the Cut Bank and Lake
458 Creek simulations.

459 **DISCUSSION**

460 **Cosmogenic exposure ages of moraines in a regional and global context**

461 The ^{10}Be exposure ages presented here for the South Fork Deep Creek (17.5 ± 0.6 ka) and
462 Cascade Creek (16.9 ± 0.1 ka) lateral moraines in the northern Absaroka Range are slightly
463 younger than ages from the previously dated lateral moraine in the neighboring Pine Creek valley
464 in the northern Absaroka (^{10}Be exposure age = 18.2 ± 0.5 ka, with the standard error of ages
465 recalculated from Licciardi and Pierce, 2008). Although these moraines were deposited by discrete
466 valley glaciers, their exposure ages are similar to ^{10}Be exposure age of the nearby Eightmile
467 terminal moraine (17.9 ± 0.4 ka, recalculated from Licciardi and Pierce, 2008), the outermost
468 moraine of the last glaciation deposited by the northern outlet glacier of the Yellowstone Icecap,
469 as well as to the age of the Chico moraine (17.1 ± 0.6 ka recalculated from Licciardi and Pierce,
470 2008) the initial moraine deposited during recession of this outlet glacier. These ages for outermost
471 and initial recessional moraine northern Yellowstone/northern Absaroka Range area in
472 southwestern Montana are also very similar to those we report here for the terminal (17.2 ± 0.2 ka)
473 and initial recessional (16.4 ± 0.2 ka) moraines at Cut Bank Creek in northwestern Montana. Taken
474 together, these ages suggest that terminal moraines in western Montana were occupied until ca.
475 18-17 ka and that glaciers were still near their maximum lengths at ca. 17-16 ka in northern
476 Yellowstone and in the Lewis Range, as indicated by exposure ages of the recessional moraines.

477 Moraines in the northern Absaroka Range have exposure ages that fall within the middle
478 Pinedale interval, 18-16 ka, as identified in the greater Yellowstone region by Licciardi and Pierce
479 (2018) and after the end of the global LGM (Clark et al., 2009). During this time, the Yellowstone

https://doi.org/10.5194/cp-2021-106
Preprint. Discussion started: 10 September 2021
© Author(s) 2021. CC BY 4.0 License.


480 glacier system thickened across the Yellowstone Plateau, coalesced with ice masses in some
481 neighboring mountains (such as the Beartooth, High Absaroka, and Gallatin Ranges), and formed
482 large outlet lobes, including the northern outlet that terminated just south of the glaciated portion
483 of the Northern Absaroka Range (Licciardi and Pierce, 2008, 2018). This large glacier system
484 persisted after the southwestern margin of the Laurentide Ice Sheet in northern Montana began
485 retreating (Dalton et al., 2020) and middle latitudes in the northern hemisphere began warming
486 (Shakun et al., 2015). Licciardi and Pierce (2018) suggest that enhanced westerly airflow into the
487 region during the middle Pinedale interval combined with orographic effects of the thickened ice
488 cap augmented precipitation in the northern Yellowstone region. The strengthened westerly
489 airflow across the region likely impacted valley glaciers in the northern Absaroka Range,
490 providing sufficient moisture for glaciers to persist at their maximum lengths despite rising
491 summer insolation at middle latitudes (Laskar et al., 2004) and atmospheric carbon dioxide
492 concentrations (Luthi et al., 2008). Additionally, middle latitudes in North America may have
493 remained cold for several millennia after the Laurentide Ice Sheet began retreating, as suggested
494 by the persistence of other Rocky Mountain glaciers at near-maximum extents until 17 ka (Laabs
495 et al., 2020) and model-based estimates of the regional temperatures at 17 ka (Liu et al., 2009; He,
496 2011).

497 The terminal and recessional moraines in the Lewis Range have exposure ages that also
498 fall within the middle Pinedale interval of 18-16 ka and thus may also have been responding to
499 similar climatic controls as in the Absaroka Range to the south. Alternatively, the post-LGM age
500 of these moraines could be related to the Lewis Range's proximity to the southwestern margin of
501 the Laurentide Ice Sheet. When the Shelby Lobe and other southwestern outlets of the Laurentide
502 Ice Sheet were at their maximum extent, general circulation modeling studies suggest that a large

https://doi.org/10.5194/cp-2021-106
Preprint. Discussion started: 10 September 2021
© Author(s) 2021. CC BY 4.0 License.


503 area of high atmospheric pressure developed across the western dome of ice sheet resulting in
504 anticyclonic, easterly airflow along the southern margins (Thompson et al., 1993; Bartlein et al.,
505 1998). This circulation pattern likely resulted in cold and dry climate in the Lewis Range while
506 the southwestern outlets occupied their terminal moraines. Recent reconstructions of this sector of
507 the Laurentide Ice Sheet suggest that the Shelby Lobe retreated to the northeast by ca. 17 ka
508 (Dalton et al., 2020), which may have been accompanied by a weakening of easterly, anticyclonic
509 circulation at the latitude of the Lewis Range and strengthening westerly airflow that delivered
510 moisture-laden air and enhanced precipitation in the mountains. Enhanced precipitation may have
511 resulted in glacier advance to their maximum lengths after the Laurentide Ice Sheet began to
512 retreat. This effect has been suggested by previous studies, including earlier interpretations of the
513 moraine chronologies in northern Yellowstone region (Licciardi et al., 2001) and age limits on
514 moraines elsewhere in northern interior mountains (Licciardi et al., 2004; Thackray et al., 2004).
515 Licciardi and Pierce (2018) note that the range of terminal-moraine exposure ages in the
516 Yellowstone region includes some that overlap with the early Pinedale interval of 22-18 ka, which
517 includes the latter part of the global Last Glacial Maximum when some southwestern outlets of
518 the Laurentide Ice Sheet were at their maximum size. While the effect of the southwestern
519 Laurentide on regional airflow may not have impacted the Yellowstone region, it may have
520 impacted the Lewis Range as indicated by the exposure ages of the terminal and recessional
521 moraines in Cut Bank valley. Additional age limits on moraines in the Lewis Range, other
522 mountains in northwestern Montana, and the Shelby Lobe will aid in understanding the relative
523 timing of mountain and continental glaciation.

524 Considering the glacial chronologies presented here in a larger spatial context, the exposure
525 ages of terminal and recessional moraines show some consistency with mountain glacier moraines

https://doi.org/10.5194/cp-2021-106
Preprint. Discussion started: 10 September 2021
© Author(s) 2021. CC BY 4.0 License.

Climate of the Past Discussions

from elsewhere in the western United States. Elsewhere in the Rocky Mountains, moraines with age limits of ca. 18-17 ka are found in the Sawtooth Range in Idaho (Thackray et al., 2004), the Wasatch and Uinta Mountains in northern Utah, and numerous glacial valleys in the Southern Rocky Mountains in Colorado (Leonard et al., 2017a; Brugger et al., 2018, 2019; Schweinsberg et al., 2020). Where sequences of moraines are exposure-dated in the Rocky Mountains, the outermost moraines of the last glaciation generally have ages that fall within the early Pinedale interval of 22-18 ka and inner moraines (representing near-maximum glacier lengths) that fall within the middle Pinedale interval (Quirk et al., 2020; Laabs et al., 2020). This pattern is observed throughout the Rocky Mountains and suggests that the mountain glacier moraine chronology in western Montana differs from the rest of the region, such that the outermost moraines do not represent the early Pinedale interval and only represent the middle Pinedale interval. This may reflect the importance of regional climatic effects on mountain glaciation, especially the strengthening of westerly airflow and attendant moisture delivery, as described above.

Inferred paleoclimate for the last glaciation

Glacier modeling results yielded a series of P_x-T_d combinations that produced ice extents that closely matched mapping-based reconstructions of the for the Cut Bank terminal and recessional positions, and for the terminal positions in the Pine Creek and South Fork Deep Creek valleys (Figure 6). Our results, particularly at Cut Bank, broadly agree with previous inferences of regional Late Pleistocene climate, including pollen-based reconstructions and other applications of paleoglaciology (Mumma et al., 2012; Murray and Locke, 1989; Locke, 1990; Birkel et al., 2012). However, to infer changes in precipitation or temperature from our glacier modeling, one of the two variables must be limited independently (i.e., from relevant paleoclimate proxy records).

https://doi.org/10.5194/cp-2021-106
Preprint. Discussion started: 10 September 2021
© Author(s) 2021. CC BY 4.0 License.

548 In the following paragraphs, we consider the modeling results in the context of some existing
549 inferences of paleoclimate based on other proxy records in western Montana.

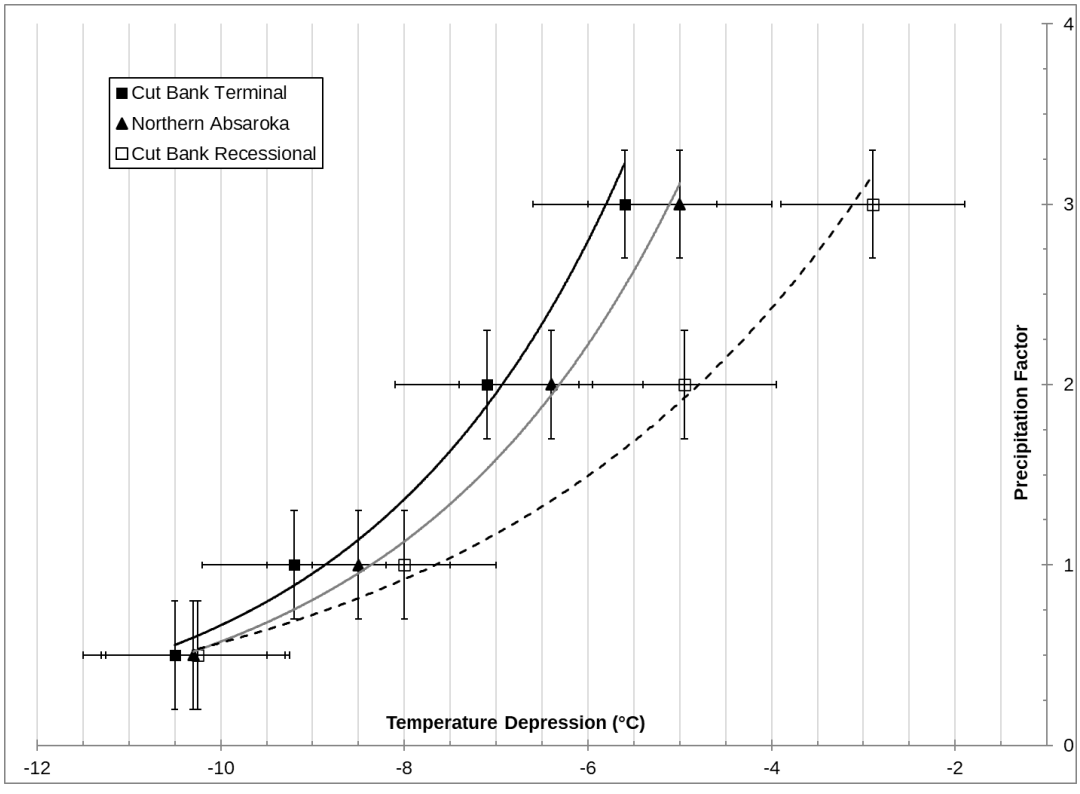

550

551 *Figure 6. Multiplicative precipitation factors and temperature depressions, both with respect to*
552 *modern, that produced modeled ice extents matching field mapped extents for 1) Cut Bank terminal*
553 *moraine 2) northern Absaroka Range Pinedale maxima at Pine Creek and South Fork Deep Creek*
554 *and 3) Cut Bank recessional moraine.*

555 Mumma et al. (2012) presented a paleoclimate record developed from Lower Red Rock
556 Lake in southwestern Montana, alongside a synthesis of other lacustrine records from the region,
557 spanning approximately from the entire LGM time interval (i.e. 26-19 ka) through the early
558 Holocene. The Lower Red Rock Lake chronology is constrained by several ^{14}C ages from organic
559 sediments and wood, plant, and peat material as well as tephrochronology. Recalibration of

https://doi.org/10.5194/cp-2021-106
Preprint. Discussion started: 10 September 2021
© Author(s) 2021. CC BY 4.0 License.


560 radiocarbon ages using IntCal20 (Reimer et al., 2020) calibration data results in changes to the
561 ages of ≤3% and therefore does not change the interpretations presented by Mumma et al. (2012).
562 Their interpretations of the pollen and sedimentological records indicate that from ca. 28-17 ka,
563 southwestern Montana was dominated by a cold and dry climate. During the subsequent interval
564 of 17.0-10.5 ka, coinciding with regional deglaciation, they suggest that temperatures increased
565 relative to the 28-17 ka period of their record but were still colder than modern and that effective
566 moisture likely increased. Mumma et al. (2012) attribute the rise in precipitation beginning at 17.0
567 ka to a northward migration of the jet stream and increasing summer insolation. Such a shift in
568 climate at 17 ka may be reflected in the glacial chronology presented here. Increased precipitation
569 commencing at 17 ka may have augmented the mass balance of mountain glaciers resulting in ice
570 advance to the terminal moraines. A glacier response to increased regional precipitation is
571 consistent with the assertion that increased westerly airflow accompanied glacier growth in the
572 Yellowstone region during the middle Pinedale interval. Alternatively, if cold and dry climate
573 during the interval 28-17 ka favored mountain glacier maxima, then the shift to warmer and wetter
574 climate at 17 ka may have initiated ice retreat from terminal moraines.

575 Reconstructions of the valley glacier that occupied Big Timber Canyon in the Crazy
576 Mountains of western Montana by Murray and Locke (1989) provide additional limits for regional
577 climate during the last glacial culmination. Their glacier model experiments, specifically the low
578 mass-balance gradients derived from them, indicate that climate in the northeastern Crazy
579 Mountains was typical of a cold, dry continental interior, with around 75% of modern precipitation,
580 when the glacier reached its maximum size, although the specific timing of the glacier maximum
581 here is unknown. Additional work by Locke (1990, 1995) on paleoglacier reconstructions suggests
582 that last-glaciation ELAs were ~450 m lower but followed a parallel trend to those of modern

https://doi.org/10.5194/cp-2021-106
Preprint. Discussion started: 10 September 2021
© Author(s) 2021. CC BY 4.0 License.


583 glacier ELAs, which he interprets to indicate similarities in temperature distributions and westerly
584 airflow across the northern Rocky Mountains of western Montana. By using the difference
585 between modern and Pleistocene ELAs to compute precipitation during the local glacial maximum
586 (for an assumed temperature depression of 10°C), Locke (1990) found that accumulation-season
587 precipitation ranged from 50 cm less than modern to 50 cm greater than modern (in units of water
588 equivalent) across mountain ranges in western Montana. However, Locke suggested that based on
589 the overall pattern of ELA change that climate in western Montana was likely drier during the
590 LGM. If precipitation changes during the last glacial culmination at 18-17 ka was 75% of modern
591 then our modeling results suggest the accompanying temperature depression in the northern
592 Absaroka Range and in the Lewis Range was around 8-10°C. The magnitude of regional climate
593 change at 18-17 ka in the Crazy Mountains is unclear, however, and may have differed between
594 the latitudes of glacial valleys in the Lewis Range (N48.6°) and that of glacial valleys in the
595 northern Absaroka (N45.5°).

596 While a unique temperature-precipitation combination for the culmination of the Pinedale
597 maximum in western Montana is difficult to infer from glacier modeling results presented here,
598 the consistent timing of the glacial culmination at 18-17 ka – after the Laurentide Ice Sheet began
599 retreating and global LGM – suggests that a regional increase in precipitation during the middle
600 Pinedale interval supported glacier maxima. This is consistent with inferred climate for the last
601 glaciation in the greater Yellowstone region described by Licciardi and Pierce (2018) and earlier
602 studies inferring that glaciers in northern mountains in the conterminous western United States
603 reached the maximum size after the Laurentide Ice Sheet began retreating (Thackray, 2008), as
604 well as the regional airflow pattern implied by the paleoglacier reconstructions of Locke (1990,
605 1995) and pollen records reported by Mumma et al. (2012). If strengthened westerly airflow at 18-

https://doi.org/10.5194/cp-2021-106
Preprint. Discussion started: 10 September 2021
© Author(s) 2021. CC BY 4.0 License.


606 17 ka resulted in accumulation-season precipitation similar to modern amounts as suggested by
607 regional climate proxies and model output, then a regional temperature depression can be inferred
608 from glacier modeling results presented here. Model simulations of glaciers in the Pine Creek and
609 South Fork Deep Creek valleys suggest a temperature depression of 8.5° ± 1.0°C in southwestern
610 Montana, whereas model simulations of the glacier in Cut Bank Creek valley suggest a temperature
611 depression of 9.2° ± 1.0°C in northwestern Montana. This magnitude of cooling for the last glacial
612 culmination in western Montana is consistent with output of some general circulation models
613 involved in the Paleoclimate Model Intercomparison Project (PMIP3), although these results
614 represent climate at 21 ka while the Laurentide Ice Sheet was still present in western Montana.
615 Specifically, the average temperature change predicted for western Montana by all PMIP3
616 ensembles is -12.9 ± 4.9 °C (1-sigma; interpolated by Oster et al., 2015).

617 **The pace of ice retreat in the Rocky Mountains**

618 Ice-margin retreat rates following the abandonment of Pinedale maximum extents in the
619 northern Rockies are constrained by the cosmogenic exposure age chronology of glacially scoured
620 and striated bedrock from Pine Creek Canyon in the northern Absaroka Range (Figure 2). First,
621 we emphasize the uncertainty associated with this deglacial chronology from the exclusion of three
622 assumed old and one young outlier from the data set. Furthermore, the sample transect only
623 captures a northern tributary of the Pine Creek glacier (see sample transect in Figure 2) and thus
624 may not be representative of the larger main-valley glacier system. However, few glaciated valleys
625 in the northern Rockies have age controls sufficient to estimate retreat rates, therefore the data
626 presented here, while limited, are valuable for inferring rates of deglaciation. Keeping these
627 considerations in mind we can use the data to describe the pattern of deglaciation in the northern
628 Absaroka.

https://doi.org/10.5194/cp-2021-106
Preprint. Discussion started: 10 September 2021
© Author(s) 2021. CC BY 4.0 License.

Climate of the Past Discussions

We model the Pine Creek glacier retreat rates using linear regressions of all or select subsets of the age and sample distance or elevation data (Figure 7). The models indicate horizontal ice-margin retreat rates ranging from 1.0 km ka^{-1} to approximately 2.6 km ka^{-1} and vertical retreat ranging from 205 to 288 m ka^{-1}. The data also suggest that the main body of ice in the Pine Creek glacier had separated from the northern tributary by ca. 16 ka, and by 13.7 ka, the northern tributary had undergone an 80% reduction in length and retreated over 1.1 km in elevation from the terminal moraine. The remaining deglacial history of the Pine Creek glacier following the inferred recession around 13.7 ka is not constrained by the cosmogenic chronology reported here.

Several studies of glaciated valleys in the western U.S. have sufficient age controls to estimate retreat rates during the last glaciation along a north-south transect of the Rocky Mountains including (Figure 8) the Pine Creek valley reported here, the Teton Range in Wyoming (Licciardi and Pierce, 2008), the Wasatch Range and Uinta Mountains in northern Utah (Laabs et al., 2011; Munroe and Laabs, 2017; Quirk et al., 2018, 2020), the Front Range (Ward et al., 2009; Duhnforth et al., 2011), Sawatch Range (Briner, 2009; Young et al., 2011; Leonard et al., 2017b; Schweinsberg et al., 2020; Tulenko et al., 2020), and San Juan Range (Guido et al., 2007) in Colorado. Here, we consider vertical retreat rates for all sites to minimize the strong effects valley slope and glacier hypsometry have on apparent rates of retreat.

Vertical glacier retreat rates exhibit no clear relationship with respect to latitude along a north-south transect from Pine Creek in southern Montana to the San Juan Rane in Colorado. Retreat rates for sites in the middle of the transect (Wasatch, Uinta, Front Range) are somewhat lower than rates calculated from the remaining sites and could reflect a response to increased moisture at these latitudes during Heinrich Stadialsl 1 (e.g. Munroe and Laabs, 2013). While the timing of initial abandonment of ice-distal positions is variable across the Rockies, ranging from

https://doi.org/10.5194/cp-2021-106
Preprint. Discussion started: 10 September 2021
© Author(s) 2021. CC BY 4.0 License.

Climate of the Past Discussions

652 the end of the LGM to ca. 16 ka, the broad pattern and timing of subsequent glacier retreat is
653 similar across the Rocky Mountains (Figure 8)

https://doi.org/10.5194/cp-2021-106
Preprint. Discussion started: 10 September 2021
© Author(s) 2021. CC BY 4.0 License.

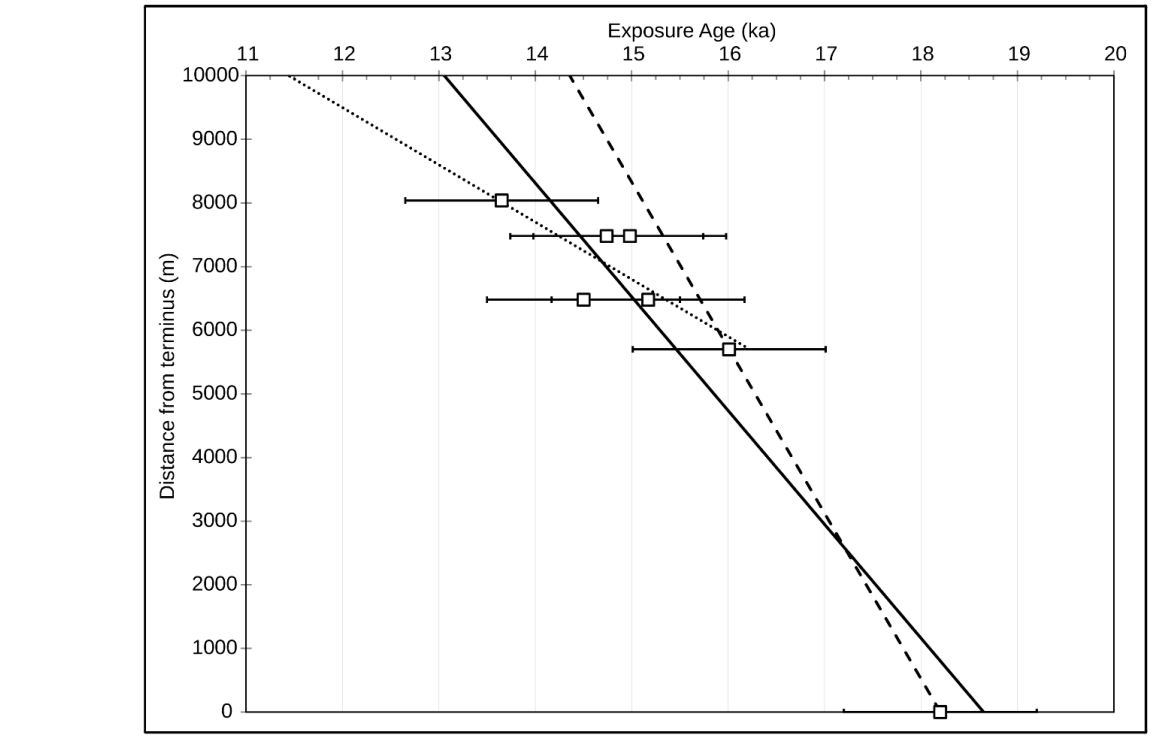

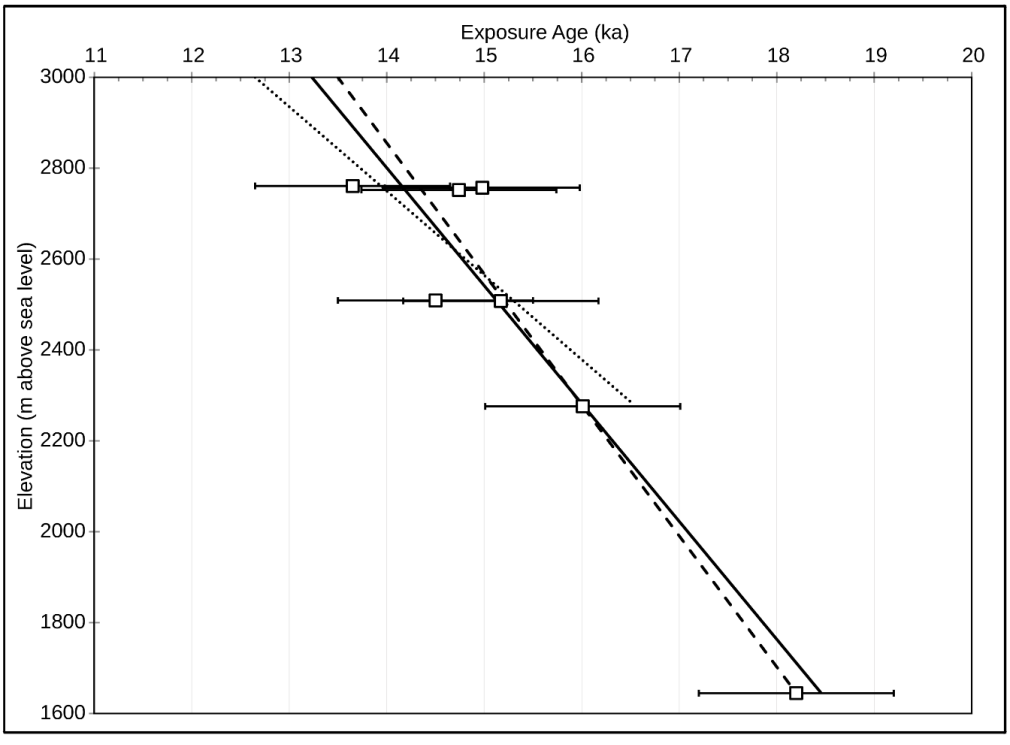

654

https://doi.org/10.5194/cp-2021-106
Preprint. Discussion started: 10 September 2021
© Author(s) 2021. CC BY 4.0 License.

Climate of the Past Discussions

Figure 7. Time-distance (top) and time-elevation (bottom) diagrams illustrating retreat from the Pine Creek Pinedale maximum extent (18.2 ± 1.3 ka; Licciardi & Pierce, 2008) from cosmogenic exposure ages collected from striated and polished bedrock along a longitudinal transect of Pine Creek. For both plots, three different retreat rates are indicated by best fit linear curves through all of the data (solid line), lateral moraine and nearest bedrock sample (dashed line), and only bedrock ages collected in this study (dotted line). All curves are extrapolated to 10 km (top) and 3000 m (bottom), which are the approximate distance to and elevation of the headwall.

The timing of terminal moraine abandonment is variable across the Rocky Mountains and span a period of around 8 ka, beginning during the LGM and continuing, such as in the Lewis and Absaroka ranges, into the middle Pinedale (18-16 ka). The large range in glacier retreat from ice-distal positions suggests diverse controlling mechanisms of initial deglaciation across the region. However, the coherence of ice-retreat rates in the Absaroka Range with locations across the Rockies from ca. 16 ka through the Lateglacial suggests common factors driving deglaciation across the region. For example, glacier retreat in Rocky Mountains after ca. 16 ka coincides with sustained increases in atmospheric CO_2 and regional temperature changes despite some glacier retreat lagging behind initial rises in CO_2 around 17 ka (Figure 8). Alternatively or in addition, modeling studies have highlighted the effect North American ice-sheets, and in particular their demise, have on regional climate (Lora et al., 2016; Tulenko et al., 2020). Specifically, the separation of the Laurentide and Cordilleran ice sheets around 15-16 ka (Dalton et al., 2020) may have led to drier and warmer conditions across Western North America (Lora et al., 2016) and thus may have contributed to sustained glacier retreat observed in the Rocky Mountains during this time period (Figure 8). Whatever the mechanism, the data presented here highlight the dramatic

https://doi.org/10.5194/cp-2021-106
Preprint. Discussion started: 10 September 2021
© Author(s) 2021. CC BY 4.0 License.

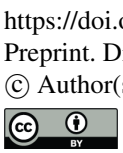

Climate of the Past Discussions
Open Access
EGU

677 age-range of initial terminal moraine abandonment and regional coherence of sustained glacier
678 retreat throughout the Lateglacial.

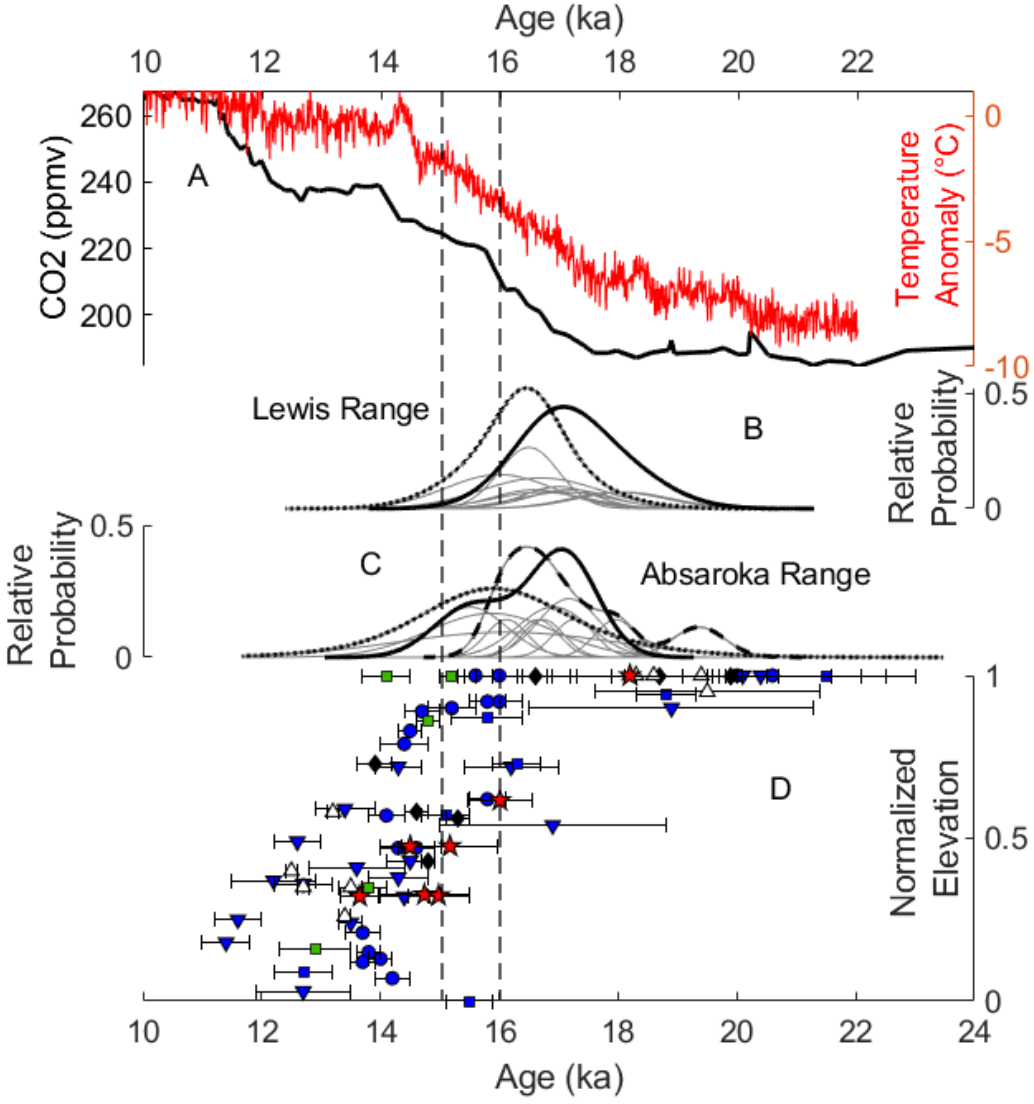

679

680 *Figure 8. (A) Surface temperature anomalies from TRACE-21ka for Western North America (red)*
681 *and Epica-Vostok composite CO_2 concentrations. (B) Camel plots of exposure age data from Cut*
682 *Bank glacier in the Lewis Range: Cut Bank terminal (solid line), Cut Bank recessional dotted line)*

https://doi.org/10.5194/cp-2021-106
Preprint. Discussion started: 10 September 2021
© Author(s) 2021. CC BY 4.0 License.


683 *and (C) Absaroka Range: South Fork Deep Creek (solid line), Cascade Creek (dotted line), and*
684 *Pine Creek (dashed line). (D) Normalized glacier elevation for Pine Creek glacier in the Absaroka*
685 *Range (red stars), Teton Range, WY (green boxes), Wasatch Range, UT (black diamonds), Uinta*
686 *Mountains, UT (white triangles), Front Range, CO (blue inverted triangles), Sawatch Range, CO*
687 *(blue circles), and San Juan Range, CO (blue squares). Dashed vertical lines bracket the*
688 *approximate timing of the separation of the Laurentide and Cordilleran ice-sheets in North*
689 *America.*

690 **CONCLUSIONS**

691 We present cosmogenic exposure ages for moraines in the Absaroka and Lewis Ranges
692 of Montana that indicate glacial stadials during the middle Pinedale interval (18-16 ka) and thus
693 after the end of the LGM. We propose that regionally strengthened westerly airflow and
694 orographic effects associated with the thickening Yellowstone Ice Cap nourished valley glaciers
695 in the Absaroka Range with precipitation and allowed glaciers to persist at their maximum
696 lengths despite rising summer insolation at middle latitudes (Laskar et al., 2004) and rising
697 atmospheric carbon dioxide concentrations (Luthi et al., 2008). Similarly in the Lewis Range,
698 glaciers maintained their maximum extents following the retreat of the Shelby Lobe of the
699 Laurentide Ice Sheet by ca. 17 ka (Dalton et al., 2020), which we propose could have been
700 accompanied by a weakening of anticyclonic circulation and strengthening of westerly airflow
701 that effectively increased precipitation in the Lewis Range. If we assume that precipitation
702 during the middle Pinedale was similar to or slightly drier than modern, following a cold and
703 likely much drier than modern early Pinedale / LGM, our model simulations of glaciers in the
704 Absaroka Range suggest a temperature depression around 8.5-9.0°C ± 1.0°C, while model
705 simulations of the Cut Bank glacier in the Lewis Range suggest a temperature depression around

https://doi.org/10.5194/cp-2021-106
Preprint. Discussion started: 10 September 2021
© Author(s) 2021. CC BY 4.0 License.


706 9.0-10.0± 1.0°C. Ice-retreat rates from Pine Creek Valley in the Absaroka Range likely ranged
707 from 1.0 to 2.6 km/ka and vertical retreat ranging from 205 to288 m ka^{-1} and broadly coincide
708 with other Rocky Mountain records of glacier retreat.

709 **CODE & DATA AVAILABILITY**

710 Cosmogenic ^{10}Be exposure age sample, AMS, and chemistry data are available in Table 1
711 and Supplemental Table 1. Glacier energy-mass balance and ice-flow model code available upon
712 request.

713 **COMPETING INTERESTS**

714 The authors declare that they have no conflict of interest.

715 **AUTHOR CONTRIBUTIONS**

716 Brendon Quirk, Elizabeth Huss, Benjamin Laabs, and Eric Leonard conceived the project
717 with input from Joseph Licciardi, and Mitchell Plummer. All listed co-authors completed field
718 mapping and sampling. Authors Quirk, Huss, and Laabs completed prep work for ^{10}Be exposure
719 dating. Marc Caffee assisted with measurement of $^{10}Be/^{9}Be$ ratios. Brendon Quirk completed all
720 glacier modeling with significant input from the other authors. All authors contributed to data and
721 modeling interpretations. Brendon Quirk and Benjamin Laabs wrote the manuscript.

722 **ACKNOWLEDGMENTS**

723 We thank the reviewers of this manuscript in advance. We also thank Doug Steen and
724 Alec Spears for help sampling the South Fork Deep Creek and Cascade Creek moraines and with
725 preliminary glacier model results.

https://doi.org/10.5194/cp-2021-106
Preprint. Discussion started: 10 September 2021
© Author(s) 2021. CC BY 4.0 License.

REFERENCES

Lora, J.M., Mitchell, J.L. and Tripati, A.E., 2016. Abrupt reorganization of North Pacific and western North American climate during the last deglaciation. Geophysical Research Letters, 43(22), pp.11-796.

Tulenko, J.P., Lofverstrom, M. and Briner, J.P., 2020. Ice sheet influence on atmospheric circulation explains the patterns of Pleistocene alpine glacier records in North America. Earth and Planetary Science Letters, 534, p.116115.

Alden, W.C., 1932. Physiography and glacial geology of eastern Montana and adjacent areas (No. 174). US Government Printing Office.

Balco, G., Stone, J.O., Lifton, N.A. and Dunai, T.J., 2008. A complete and easily accessible means of calculating surface exposure ages or erosion rates from 10 Be and 26 Al measurements. Quaternary geochronology, v. 3, p. 174-195.

Birkel S.D., Putnam A.E., Denton G.H., Koons P.O., Fastook J.L., Putnam D.E., Maasch, K.A. 2012. Climate inferences from a glaciological reconstruction of the late Pleistocene Wind River ice cap, Wind River Range, Wyoming. Arctic, Antarctic, and Alpine research 44, 265-76. doi:10.1657/1938-4246-44.3.265.

Blackwelder, E., 1931. Pleistocene glaciation in the Sierra Nevada and Basin ranges. Bulletin of the Geological Society of America, 42(4), pp.865-922.

Borchers, B., Marrero, S., Balco, G., Caffee, M., Goehring, B., Lifton, N., Nishiizumi, K., Phillips, F., Schaefer, J. and Stone, J., 2016. Geological calibration of spallation production rates in the CRONUS-Earth project. Quaternary Geochronology, v. 31, p. 188-198.

Briner, J.P., 2009. Moraine pebbles and boulders yield indistinguishable 10Be ages: a case study from Colorado, USA. Quaternary Geochronology, 4(4), pp.299-305.

https://doi.org/10.5194/cp-2021-106
Preprint. Discussion started: 10 September 2021
© Author(s) 2021. CC BY 4.0 License.


749 Brugger, K.A.; Laabs, B.; Reimers, A.; Bensen, N., 2018. Late Pleistocene glaciation in the
750 Mosquito Range, Colorado, USA: Chronology and climate. Journal of Quaternary Science,
751 *34*, 187–202.
752 Brugger, K.A., Ruleman, C.A., Caffee, M.W., Mason, C.C., 2019. Climate during the Last
753 Glacial Maximum in the Northern Sawatch Range, Colorado. Quaternary 2, 36.
754 doi:10.3390/quat2040036.
755 Calhoun, F.H.H., 1906. The Montana lobe of the Keewatin ice sheet.. (No. 50). The University of
756 Chicago Press.
757 Carrara, P.E., 1989. Late Quaternary glacial and vegetative history of the Glacier National Park
758 region, Montana (No. 1902). USGPO; For sale by the Books and Open-File Reports Section,
759 US Geological Survey.
760 Clark, P.U., Dyke, A.S., Shakun, J.D., Carlson, A.E., Clark, J., Wohlfarth, B., Mitrovica, J.X.,
761 Hostetler, S.W. and McCabe, A.M., 2009. The last glacial maximum. Science, v. 325, p. 710-
762 714.
763 Dalton, A.S., Margold, M., Stokes, C.R., Tarasov, L., Dyke, A.S., Adams, R.S., Allard, S., Arends,
764 H.E., Atkinson, N., Attig, J.W. and Barnett, P.J., 2020. An updated radiocarbon-based ice
765 margin chronology for the last deglaciation of the North American Ice Sheet Complex.
766 Quaternary Science Reviews, 234, p.106223.
767 Daly, C., Halbleib, M., Smith, J.I., Gibson, W.P., Doggett, M.K., Taylor, G.H., Curtis, J. and
768 Pasteris, P.P., 2008. Physiographically sensitive mapping of climatological temperature and
769 precipitation across the conterminous United States. International journal of climatology, v.
770 28, p. 2031-2064.

https://doi.org/10.5194/cp-2021-106
Preprint. Discussion started: 10 September 2021
© Author(s) 2021. CC BY 4.0 License.


771 Dühnforth, M. and Anderson, R.S., 2011. Reconstructing the glacial history of green lakes valley,
772 North Boulder Creek, Colorado Front Range. Arctic, Antarctic, and Alpine Research, 43(4),
773 pp.527-542.
774 Fastook, J.L. and Chapman, J.E., 1989. A map-plane finite-element model: three modeling
775 experiments. Journal of Glaciology, v. 35, p. 48-52.
776 Guido, Z.S., Ward, D.J. and Anderson, R.S., 2007. Pacing the post–Last Glacial Maximum demise
777 of the Animas Valley glacier and the San Juan Mountain ice cap, Colorado. Geology, 35(8),
778 pp.739-742.
779 Harrison, S., Rowan, A.V., Glasser, N.F., Knight, J., Plummer, M.A. and Mills, S.C., 2014. Little
780 Ice Age glaciers in Britain: Glacier–climate modelling in the Cairngorm mountains. The
781 Holocene, v. 24, p. 135-140.
782 Heinrich, H., 1988. Origin and consequences of cyclic ice rafting in the northeast Atlantic Ocean
783 during the past 130,000 years. Quaternary Research, v. 29, p. 142-152.
784 Kohl, C.P. and Nishiizumi, K., 1992. Chemical isolation of quartz for measurement of in-situ-
785 produced cosmogenic nuclides. Geochimica et Cosmochimica Acta, 56(9), pp.3583-3587.
786 Laabs, B.J., Marchetti, D.W., Munroe, J.S., Refsnider, K.A., Gosse, J.C., Lips, E.W., Becker, R.A.,
787 Mickelson, D.M. and Singer, B.S., 2011. Chronology of latest Pleistocene mountain glaciation
788 in the western Wasatch Mountains, Utah, U.S.A., Quaternary Research, v. 76, p. 272-284.
789 Laabs, B.J., Munroe, J.S., Best, L.C. and Caffee, M.W., 2013. Timing of the last glaciation and
790 subsequent deglaciation in the Ruby Mountains, Great Basin, USA. Earth and Planetary
791 Science Letters, v. 361, p. 16-25.

https://doi.org/10.5194/cp-2021-106
Preprint. Discussion started: 10 September 2021
© Author(s) 2021. CC BY 4.0 License.


792 Laabs, B.J., Plummer, M.A. and Mickelson, D.M., 2006. Climate during the last glacial maximum
793 in the Wasatch and southern Uinta Mountains inferred from glacier modeling.
794 Geomorphology, v. 75, p. 300-317.
795 Laabs, B.J.C., and Munroe, J.S., 2016. Late Pleistocene mountain glaciation in the Lake
796 Bonneville Basin, In Oviatt, C.G., and Schroeder, J., Lake Bonneville: A Scientific Update,
797 Elsevier, Amsterdam, The Netherlands, p. 462-503.
798 Leonard, E.M., 1989, Climatic change in the Colorado Rocky Mountains: estimates based on modern
799 climate at late Pleistocene equilibrium lines: *Arctic and Alpine Research* 21, 245-255.
800 Leonard, E.M., Plummer, M.A., Carrara, P.E., 2014, Numerical modeling of the Snowmass
801 Creek paleoglacier, Colorado: implications for climate in the Rocky Mountains during the
802 Bull Lake glaciation (MIS 6). Quaternary Research 82, 533-541. doi:
803 10.1016/j.yqres.2014.03.001.
804 Leonard, E.M., Laabs, B.J., Plummer, M.A., Kroner, R.K., Brugger, K.A., Spiess, V.M.,
805 Refsnider, K.A., Xia, Y. and Caffee, M.W., 2017a. Late Pleistocene glaciation and deglaciation
806 in the Crestone Peaks area, Colorado Sangre de Cristo Mountains, USA–chronology and
807 paleoclimate. Quaternary Science Reviews, v. 158, p. 127-144.
808 Leonard, E.M., Laabs, B.J., Schweinsberg, A.D., Russell, C.M., Briner, J.P., Young, N.E., 2017b.
809 Glaciation in the Colorado Rocky Mountains, USA, following the last glacial maximum.
810 *Cuadernos de Investigación Geográfica* 43, 497-526. http://doi.org/10.18172/cig.3234
811 Licciardi, J.M. and Pierce, K.L., 2008. Cosmogenic exposure-age chronologies of Pinedale and
812 Bull Lake glaciations in greater Yellowstone and the Teton Range, USA. Quaternary Science
813 Reviews, 27(7-8), pp.814-831.

https://doi.org/10.5194/cp-2021-106
Preprint. Discussion started: 10 September 2021
© Author(s) 2021. CC BY 4.0 License.


814 Licciardi, J.M. and Pierce, K.L., 2018. History and dynamics of the Greater Yellowstone Glacial
815 System during the last two glaciations. Quaternary Science Reviews, 200, pp.1-33.
816 Licciardi, J.M., Clark, P.U., Brook, E.J., Pierce, K.L., Kurz, M.D., Elmore, D. and Sharma, P.,
817 2001. Cosmogenic 3He and 10Be chronologies of the late Pinedale northern Yellowstone ice
818 cap, Montana, USA. Geology, 29(12), pp.1095-1098.
819 Lifton, N., Caffee, M., Finkel, R., Marrero, S., Nishiizumi, K., Phillips, F.M., Goehring, B., Gosse,
820 J., Stone, J., Schaefer, J. and Theriault, B., 2015. In situ cosmogenic nuclide production rate
821 calibration for the CRONUS-Earth project from Lake Bonneville, Utah, shoreline features.
822 Quaternary Geochronology, v. 26, p. 56-69.
823 Lifton, N., Sato, T. and Dunai, T.J., 2014. Scaling in situ cosmogenic nuclide production rates
824 using analytical approximations to atmospheric cosmic-ray fluxes. Earth and Planetary Science
825 Letters, v. 386, p. 149-160.
826 Locke, W.W., 1990. Late Pleistocene glaciers and the climate of western Montana, USA. *Arctic*
827 *and Alpine Research* 22, 1-13.
828 Locke, W.W., 1995. Modelling of icecap glaciation of the northern Rocky Mountains of
829 Montana. Geomorphology 14, pp.123-130.
830 McCoy, W.D., Williams, L.D., Kay, P.A. and Diaz, H.F., 1985. Application of an energy-balance
831 model to the late Pleistocene Little Cottonwood Canyon glacier with implications regarding
832 the paleohydrology of Lake Bonneville. Problems of and prospects for predicting Great Salt
833 Lake levels: Salt Lake City, University of Utah, pp.40-53.
834 Munroe, J.S. and Laabs, B.J., 2017. Combining radiocarbon and cosmogenic ages to constrain the
835 timing of the last glacial-interglacial transition in the Uinta Mountains, Utah, USA. Geology,
836 45(2), pp.171-174.

https://doi.org/10.5194/cp-2021-106
Preprint. Discussion started: 10 September 2021
© Author(s) 2021. CC BY 4.0 License.


837 Murray and Locke, 1989

838 Muzikar, P., Elmore, D. and Granger, D.E., 2003. Accelerator mass spectrometry in geologic
839 research. Geological Society of America Bulletin, v. 115, p. 643-654.

840 Oerlemans, J., 1989. On the response of valley glaciers to climatechange. In: Oerlemans, J. (Ed.),
841 Glacier Fluctuations and Climate Change. Reidel, Dordrecht, p. 353– 371.

842 Osborn, G. and Bevis, K., 2001. Glaciation in the Great Basin of the western United States.
843 Quaternary Science Reviews, v. 20, p. 1377-1410.

844 Oster, J.L., Ibarra, D.E., Winnick, M.J. and Maher, K., 2015. Steering of westerly storms over
845 western North America at the Last Glacial Maximum. Nature Geoscience, v.8, p.201.

846 Petit, J.R., Jouzel, J., Raynaud, D., Barkov, N.I., Barnola, J.M., Basile, I., Bender, M., Chappellaz,
847 J., Davis, M., Delaygue, G. and Delmotte, M., 1999. Climate and atmospheric history of the
848 past 420,000 years from the Vostok ice core, Antarctica. Nature, v. 399, p. 429.

849 Pierce, K.L., 1973. Surficial geologic map of the Mammoth quadrangle and part of the Gardiner
850 quadrangle, Yellowstone National Park, Wyoming and Montana (No. 641).

851 Pierce, K.L., 1979. History and dynamics of glaciation in the northern Yellowstone National Park
852 area: US Geol. Survey Prof. Paper.

853 Plummer, M.A., Phillips, F.M., 2003. A 2-D numerical model of snow/ice energy balance and ice
854 flow for paleoclimatic interpretation of glacial geomorphic features. Quaternary Science
855 Reviews, v. 22, p. 1389-1406.

856 Putnam, A.E., Denton, G.H., Schaefer, J.M., Barrell, D.J., Andersen, B.G., Finkel, R.C., Schwartz,
857 R., Doughty, A.M., Kaplan, M.R. and Schlüchter, C., 2010. Glacier advance in southern
858 middle-latitudes during the Antarctic Cold Reversal. Nature Geoscience, 3(10), pp.700-704.

https://doi.org/10.5194/cp-2021-106
Preprint. Discussion started: 10 September 2021
© Author(s) 2021. CC BY 4.0 License.


859 Quirk, B. J., Moore, J. R., Laabs, B. J., Caffee, M. W., Plummer, M. A., 2018. Termination II,
860 Last Glacial Maximum, and Lateglacial chronologies and paleoclimate from Big Cottonwood
861 Canyon, Wasatch Mountains, Utah. *Geological Society of America Bulletin* 130, 1889-1902.
862 doi:10.1030/B31967.1.
863 Quirk, B. J., Moore, J. R., Laabs, B. J., Plummer, M. A., Caffee, M. W., 2020, Latest Pleistocene
864 glacial and climate history of the Wasatch Range, Utah. Quaternary Science Reviews 238,
865 106313, 1-17. Doi: 10.1016/j.quascirev.2020.106313.
866 Reimer, P.J., Austin, W.E., Bard, E., Bayliss, A., Blackwell, P.G., Ramsey, C.B., Butzin, M.,
867 Cheng, H., Edwards, R.L., Friedrich, M. and Grootes, P.M., 2020. The IntCal20 Northern
868 Hemisphere radiocarbon age calibration curve (0–55 cal kBP). Radiocarbon, 62(4), pp.725-
869 757.Rowan, A.V., Brocklehurst, S.H., Schultz, D.M., Plummer, M.A., Anderson, L.S. and
870 Glasser, N.F., 2014. Late Quaternary glacier sensitivity to temperature and precipitation
871 distribution in the Southern Alps of New Zealand. Journal of Geophysical Research: Earth
872 Surface, v. 119, p. 1064-1081.
873 Schweinsberg, A.D., Briner, J.P., Licciardi, J.M., Shroba, R.R., Leonard, E.M., 2020.
874 Cosmogenic ^{10}Be exposure dating of Bull Lake and Pinedale glaciations and
875 deglaciation in the upper Arkansas River valley, Colorado Rocky Mountains, U.S.A.
876 *Quaternary Research* 97. http://doi: 10.1017/qua.2020.21.
877 Shakun, J.D., Clark, P.U., He, F., Lifton, N.A., Liu, Z. and Otto-Bliesner, B.L., 2015. Regional
878 and global forcing of glacier retreat during the last deglaciation. Nature communications, v. 6.
879 Thackray, G.D., 2008. Varied climatic and topographic influences on Late Pleistocene mountain
880 glaciation in the western United States. Journal of Quaternary Science, v. 23, p.671-681.

https://doi.org/10.5194/cp-2021-106
Preprint. Discussion started: 10 September 2021
© Author(s) 2021. CC BY 4.0 License.


881 Thackray, G.D., Lundeen, K.A. and Borgert, J.A., 2004. Latest Pleistocene alpine glacier advances
882 in the Sawtooth Mountains, Idaho, USA: reflections of midlatitude moisture transport at the
883 close of the last glaciation. Geology, 32(3), pp.225-228.
884 Uppala, S.M., Kållberg, P.W., Simmons, A.J., Andrae, U., Bechtold, V.D., Fiorino, M., Gibson,
885 J.K., Haseler, J., Hernandez, A., Kelly, G.A. and Li, X., 2005. The ERA-40 re-analysis.
886 Quarterly Journal of the royal meteorological society, v. 131, p. 2961-3012.
887 Ward, D.J., Anderson, R.S., Guido, Z.S. and Briner, J.P., 2009. Numerical modeling of
888 cosmogenic deglaciation records, Front Range and San Juan mountains, Colorado. Journal of
889 Geophysical Research: Earth Surface, 114(F1).
890 Weed, W.H., 1893. The glaciation of the Yellowstone valley north of the park (No. 104). US
891 Geological Survey.
892 Young, N.E., Briner, J.P., Leonard, E.M., Licciardi, J.M. and Lee, K., 2011. Assessing climatic
893 and nonclimatic forcing of Pinedale glaciation and deglaciation in the western United States.
894 Geology, v. 39, p. 171-174.
895